treatment with 5-Aza-CdR and PBA and after transfection of *miR-512-5p* (Figure 4c).

In addition, levels of apoptosis were evaluated by photometric enzyme-immunoassay for the detection of cytoplasmic histone-associated DNA fragments. Significant increase of the levels of cytoplasmic histone-associated DNA fragments (mono- and oligonucleosomes) was observed in AGS cells both after treatment with 5-Aza-CdR and PBA and after transfection of *miR-512-5p* (Figure 4d).

To further confirm target specificity between *miR-512-5p* and its potential target, *Mcl-1*, we carried out luciferase reporter assay with a vector containing the putative *Mcl-1* 3′ untranslated region (UTR) target site downstream of the luciferase reporter gene, which was transfected into AGS cells. Base pairing between *miR-512-5p* and wild-type (WT) or mutant (MUT) target site in the 3′ UTR of *Mcl-1* mRNA is shown in Figure 5a. Luciferase activities of AGS cells transfected with Mcl-1-WT construct were significantly lower after epigenetic treatment and after transfection of *miR-512-5p*, whereas those with Mcl-1-MUT construct showed no significant difference (Figure 5b). These data suggest that *Mcl-1* is one of the targets of *miR-512-5p* and that activation of *miR-512-5p* induces suppression of *Mcl-1*, resulting in apoptosis of gastric cancer cells.

Discussion

Alu repeats are the most frequent repetitive elements in the human genome and have been considered as 'junk DNA' with no important function. However, Borchert *et al.* (2006) have shown that Alu repeats in the miRNA cluster on chromosome 19 can function as Pol III promoters of downstream miRNAs. These Alu-associated miRNAs are shown to be silenced in the human tissues except the placenta (Bentwich *et al.*, 2005). We also found that Alu-associated miRNAs are silenced in both gastric cancers and non-cancerous mucosae (data not shown).

In this study, we show that one of the Alu-associated miRNAs, *miR-512-5p*, is silenced by epigenetic mechanisms, and that chromatin remodeling at Alu repeats by DNA methylation inhibitors and HDAC inhibitors can activate expression of silenced *miR-512-5p* in human gastric cancer cells. The DNA demethylating agent 5-Aza-CdR and HDAC inhibitor PBA were effective at reducing DNA methylation level and activating chromatin structure at the promoter region of *miR-512-5p*. In agreement with our results, earlier studies have suggested that Alu transcription is regulated by epigenetic mechanisms such as DNA methylation and histone modification at Alu repeats (Liu *et al.*, 1994; Kondo and Issa, 2003).

Although it has been reported that Alu-associated miRNAs are transcribed by Pol III (Borchert *et al.*, 2006), our results suggest that epigenetic activation of *miR-512-5p* is mediated by Pol II. Interestingly, Alu elements on the promoter region of *miR-512-5p* are separated from mature *miR-512-5p* sequences by Pol III terminator (TTTT), indicating that Pol III at Alu elements cannot transcribe *miR-512-5p* (Figure 2a). This finding supports our results that chromatin remodeling by epigenetic treatment at Alu repeats can activate *miR-512-5p* through Pol II. A recent study also reports about Pol II transcription associated with Alu repeats and CpG islands in human promoters (Oei *et al.*, 2004).

Gastric cancer is the second most common cause of cancer-related death worldwide. Although the incidence of gastric cancer has declined in western countries, it remains a major health problem throughout the rest of the world, especially in China and Japan (Parkin, 2001).

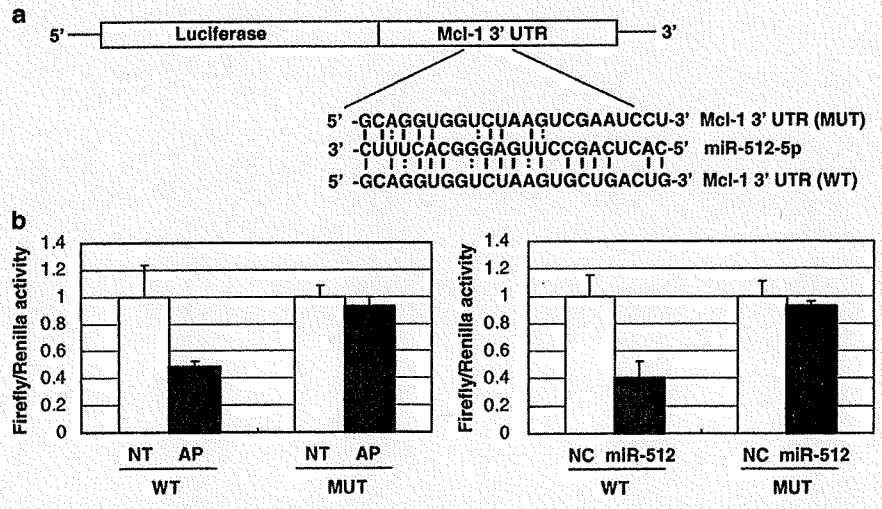

Figure 5 Identification of *Mcl-1* as a target of *miR-512-5p*. (a) Luciferase reporter constructs containing wild-type (WT) or mutant (MUT) target site of the 3′ untranslated region (UTR) of *Mcl-1* mRNA. (b) The firefly luciferase activity normalized to the *Renilla* luciferase activity in AGS cells not treated (NT) or treated with 5-aza-2′-deoxycytidine and 4-phenylbutyric acid (AP) and in AGS cells transfected with negative control (NC) or *miR-512-5p* precursor molecules (miR-512).

For gastric cancer that is diagnosed at an advanced stage, systemic chemotherapy is the only treatment available, besides supportive care. The *Mcl-1* gene is a member of the *Bcl-2* family and an anti-apoptotic protein originally isolated from the ML-1 human myeloid leukemia cell line during cell differentiation (Kozopas *et al.*, 1993). The biological relevance of Mcl-1 as an anti-apoptotic protein promoting cell survival has been reported in various human malignancies (Zhou *et al.*, 1997; Shigemasa *et al.*, 2002; Taniai *et al.*, 2004). Elevated expression of *Mcl-1* and its association with poor prognosis have been reported in gastric cancer (Krajewska *et al.*, 1996; Maeta *et al.*, 2004). Interestingly, Wacheck *et al.* (2006) have proposed *Mcl-1* antisense therapy as a promising approach for the treatment of gastric cancer. They have shown that downregulation of *Mcl-1* by antisense therapy produced a significant increase in apoptosis and a decrease in cell growth, and that the combination of *Mcl-1* antisense oligonucleotide and anti-cancer agents, such as docetaxel and cisplatin, showed synergistic chemopreventive activity (Wacheck *et al.*, 2006; Zangemeister-Wittke and Huwiler, 2006). Our results show that activation of *miR-512-5p* induced by chromatin-modifying drugs suppresses *Mcl-1*, resulting in apoptosis of gastric cancer cells. In addition, activation of Alu-associated miRNAs by epigenetic treatment seems to be more specific in gastric cancer cells compared with bladder cancer cells. These results indicate that Alu-associated miRNAs could be novel therapeutic targets of human gastric cancer.

In conclusion, our results suggest that chromatin remodeling at Alu repeats by DNA demethylation and HDAC inhibition can induce expression of silenced miRNAs, which can serve as 'endogenous silencers' of target oncogenes in gastric cancer cells. As there is a possibility that other proteins activated by epigenetic treatment may also contribute to apoptosis in gastric cancer cells, further studies are necessary to verify whether activation of Alu-associated miRNAs by epigenetic therapy could be an effective approach for the prevention and treatment of human gastric cancer.

Materials and methods

Cell lines and epigenetic treatment
The AGS, MKN45 and TMK1 human gastric cancer cell lines were used. AGS was obtained from the American Type Culture Collection (Rockville, MD, USA), and MNK45 was obtained from the Japan Health Science Foundation (Osaka, Japan). TMK1 is a generous gift from Dr Wataru Yasui (Ochiai *et al.*, 1985). Cells were cultured in RPMI1640 medium supplemented with 10% fetal bovine serum. They were seeded at 24 h before treatment with 5-Aza-CdR (Sigma-Aldrich, St Louis, MO, USA) and PBA (Sigma-Aldrich). 5-Aza-CdR was removed after 24 h, whereas the cells were continuously exposed to PBA for 96 h.

RNA extraction and microarray analyses
Total RNA, including small RNA, was extracted using the mirVana miRNA isolation kit (Ambion, Austin, TX, USA). miRNA microarray analysis was carried out by LC Sciences (www.lcsciences.com, Houston, TX, USA), and gene expression profile was analysed using the whole human genome oligo microarray kit (Agilent technologies, Santa Clara, CA, USA). All data were submitted to the ArrayExpress database, and the accession numbers are E-MEXP-1820 and E-MEXP-1821, respectively.

Quantitative RT–PCR of miRNAs
MicroRNA expression levels were analysed by quantitative RT–PCR using the TaqMan microRNA assay for *miR-512-5p, -515-5p, -517b, -518b* and *-526b* (Applied Biosystems, Foster City, CA, USA), in accordance with the manufacturer's instructions.

Bisulfite genomic sequencing
Genomic DNA was converted with sodium bisulfite. After amplification of the bisulfite-converted DNA by nested PCR with specific primers for *miR-512*, DNA methylation levels were analysed by bisulfite genomic sequencing as described earlier (Saito *et al.*, 2006). The sequences of the primers used are listed in Supplementary Table 1.

Chromatin immunoprecipitation assay
The ChIP assay was carried out as described earlier (Saito *et al.*, 2006). Antibodies to dimethylated histone H3-K4 (Upstate, Temecula, CA, USA), acetylated histone H3 (Upstate), Pol II (Upstate) and Pol III (anti-RPC 53, see Acknowledgements) were used. Quantitative analysis was carried out by real-time PCR with the CYBR Premix Ex Taq (Takara Bio, Ohtsu, Japan) using the Thermal Cycler Dice Real-Time System (Takara Bio). The sequences of the primers used are listed in Supplementary Table 1. The fraction of immunoprecipitated DNA was calculated as follows: (immunoprecipitated DNA with each antibody−nonspecific antibody control (NAC))/(input DNA–NAC).

5′-Rapid amplification of cDNA ends
5′ ends of mRNA were detected using the RLM-RACE kit (Ambion) according to the manufacturer's protocols. The inner 5′ RLM-RACE PCR products were cut from 2% agarose gel, purified using Gel Extraction Kit (Qiagen, Tokyo, Japan) and sequenced with an inner gene-specific primer. The sequences of the primers used are listed in Supplementary Table 1.

Western blotting and quantitative RT–PCR
Protein extracts were separated by SDS/polyacrylamide gel electrophoresis and transferred onto a nitrocellulose membrane. Membranes were hybridized with antibodies against Mcl-1 (S-19, Santa Cruz Biotechnology, Santa Cruz, CA, USA).

Total RNA was used for reverse transcription. After incubation with DNase I (Promega, Madison, WI, USA) to eliminate DNA contamination, Superscript III (Invitrogen, Carlsbad, CA, USA) and random hexamers (Invitrogen) were added for first-strand cDNA synthesis, then, quantitative PCR was carried out with primers specific for *Jun* and *Mcl-1* (Supplementary Table 1).

Transfection of miR-512-5p *precursor molecules*
The *miR-512-5p* precursor molecules and negative control 1 precursor miRNAs were purchased from Ambion. They were transfected into AGS cells at a final concentration of 100 nM each using oligofectamine (Invitrogen), in accordance with the manufacturer's instructions. At 48 h after transfection, cells were collected and the expression of Mcl-1 was analysed by western blotting as described above.

Apoptosis assay
AGS cells were transfected with *miR-512-5p* and negative control or treated with 5-Aza-CdR and PBA. Forty-eight hours later, apoptosis was evaluated by photometric enzyme-immunoassay for the detection of cytoplasmic histone-associated DNA fragments using the Cell Death Detection ELISA kit (Roche, Mannheim, Germany) (Suzuki *et al.*, 1998).

Luciferase assay
Luciferase constructs were made by ligating oligonucleotides containing the wild-type or mutant target site of the *Mcl-1* 3′ UTR into the *Xba* I site of the pGL3-control vector (Promega, Figure 5a). AGS cells were transfected with 0.4 μg of firefly luciferase reporter vector containing wild-type or mutant target site and 0.02 μg of the control vector containing *Renilla* luciferase, pRL-CMV (Promega), using lipofectamine 2000 (Invitrogen) in 24-well plates. Luciferase assays were carried out at 48 h after transfection using the Dual Luciferase Reporter Assay System (Promega). Firefly luciferase activity was normalized to *Renilla* luciferase activity.

Conflict of interest

Dr Saito's work has been funded by a Grant-in-Aid for Scientific Research from the Japan Society for the Promotion of Science (JSPS). Dr Suzuki's work has been funded by a Grant-in-Aid for Exploratory Research from the JSPS. Dr Kanai's work has been funded by the Ministry of Health, Labor and Welfare of Japan. Dr Hibi's work has been funded by the JSPS and the Ministry of Education, Culture, Sports, Science and Technology.

Acknowledgements

The authors are grateful to Dr Robert Roeder at Rockefeller University for providing antibody to Pol III. This work was supported by a Grant-in-Aid for Scientific Research C from the Japan Society for the Promotion of Science (JSPS) (19599024, to Y.S.) and a Grant-in-Aid for Exploratory Research from JSPS (19659057, to HS).

References

Bagga S, Bracht J, Hunter S, Massirer K, Holtz J, Eachus R *et al.* (2005). Regulation by let-7 and lin-4 miRNAs results in target mRNA degradation. *Cell* **122**: 553–563.

Bentwich I, Avniel A, Karov Y, Aharonov R, Gilad S, Barad O *et al.* (2005). Identification of hundreds of conserved and nonconserved human microRNAs. *Nat Genet* **37**: 766–770.

Borchert GM, Lanier W, Davidson BL. (2006). RNA polymerase III transcribes human microRNAs. *Nat Struct Mol Biol* **13**: 1097–1101.

Calin GA, Croce CM. (2006a). MicroRNA signatures in human cancers. *Nat Rev Cancer* **6**: 857–866.

Calin GA, Croce CM. (2006b). MicroRNAs and chromosomal abnormalities in cancer cells. *Oncogene* **25**: 6202–6210.

Esteller M. (2002). CpG island hypermethylation and tumor suppressor genes: a booming present, a brighter future. *Oncogene* **21**: 5427–5440.

Gal-Yam EN, Saito Y, Egger G, Jones PA. (2008). Cancer epigenetics: modifications, screening, and therapy. *Annu Rev Med* **59**: 267–280.

Kondo Y, Issa JP. (2003). Enrichment for histone H3 lysine 9 methylation at Alu repeats in human cells. *J Biol Chem* **278**: 27658–27662.

Kozopas KM, Yang T, Buchan HL, Zhou P, Craig RW. (1993). MCL1, a gene expressed in programmed myeloid cell differentiation, has sequence similarity to BCL2. *Proc Natl Acad Sci USA* **90**: 3516–3520.

Krajewska M, Fenoglio-Preiser CM, Krajewski S, Song K, Macdonald JS, Stemmerman G *et al.* (1996). Immunohistochemical analysis of Bcl-2 family proteins in adenocarcinomas of the stomach. *Am J Pathol* **149**: 1449–1457.

Liu WM, Maraia RJ, Rubin CM, Schmid CW. (1994). Alu transcripts: cytoplasmic localisation and regulation by DNA methylation. *Nucleic Acids Res* **22**: 1087–1095.

Maeta Y, Tsujitani S, Matsumoto S, Yamaguchi K, Tatebe S, Kondo A *et al.* (2004). Expression of Mcl-1 and p53 proteins predicts the survival of patients with T3 gastric carcinoma. *Gastric Cancer* **7**: 78–84.

Ochiai A, Yasui W, Tahara E. (1985). Growth-promoting effect of gastrin on human gastric carcinoma cell line TMK-1. *Jpn J Cancer Res* **76**: 1064–1071.

Oei SL, Babich VS, Kazakov VI, Usmanova NM, Kropotov AV, Tomilin NV. (2004). Clusters of regulatory signals for RNA polymerase II transcription associated with Alu family repeats and CpG islands in human promoters. *Genomics* **83**: 873–882.

Parkin DM. (2001). Global cancer statistics in the year 2000. *Lancet Oncol* **2**: 533–543.

Saito Y, Jones PA. (2006). Epigenetic activation of tumor suppressor microRNAs in human cancer cells. *Cell Cycle* **5**: 2220–2222.

Saito Y, Liang G, Egger G, Friedman JM, Chuang JC, Coetzee GA *et al.* (2006). Specific activation of microRNA-127 with down-regulation of the proto-oncogene BCL6 by chromatin-modifying drugs in human cancer cells. *Cancer Cell* **9**: 435–443.

Shigemasa K, Katoh O, Shiroyama Y, Mihara S, Mukai K, Nagai N *et al.* (2002). Increased MCL-1 expression is associated with poor prognosis in ovarian carcinomas. *Jpn J Cancer Res* **93**: 542–550.

Suzuki H, Seto K, Mori M, Suzuki M, Miura S, Ishii H. (1998). Monochloramine induced DNA fragmentation in gastric cell line MKN45. *Am J Physiol* **275**: G712–G716.

Taniai M, Grambihler A, Higuchi H, Werneburg N, Bronk SF, Farrugia DJ *et al.* (2004). Mcl-1 mediates tumor necrosis factor-related apoptosis-inducing ligand resistance in human cholangiocarcinoma cells. *Cancer Res* **64**: 3517–3524.

Wacheck V, Cejka D, Sieghart W, Losert D, Strommer S, Crevenna R *et al.* (2006). Mcl-1 is a relevant molecular target for antisense oligonucleotide strategies in gastric cancer cells. *Cancer Biol Ther* **5**: 1348–1354.

Wu L, Fan J, Belasco JG. (2006). MicroRNAs direct rapid deadenylation of mRNA. *Proc Natl Acad Sci USA* **103**: 4034–4039.

Yekta S, Shih IH, Bartel DP. (2004). MicroRNA-directed cleavage of HOXB8 mRNA. *Science* **304**: 594–596.

Yoo CB, Jones PA. (2006). Epigenetic therapy of cancer: past, present and future. *Nat Rev Drug Discov* **5**: 37–50.

Zangemeister-Wittke U, Huwiler A. (2006). Antisense targeting of Mcl-1 has therapeutic potential in gastric cancer. *Cancer Biol Ther* **5**: 1355–1356.

Zhou P, Qian L, Kozopas KM, Craig RW. (1997). Mcl-1, a Bcl-2 family member, delays the death of hematopoietic cells under a variety of apoptosis-inducing conditions. *Blood* **89**: 630–643.

Supplementary Information accompanies the paper on the Oncogene website (http://www.nature.com/onc)

Cancer Science
The official journal of the Japanese Cancer Association JCA

Characteristics of prostate cancers found in specimens removed by radical cystoprostatectomy for bladder cancer and their relationship with serum prostate-specific antigen level

Tohru Nakagawa,[1,3] Yae Kanai,[2] Motokiyo Komiyama,[1] Hiroyuki Fujimoto[1] and Tadao Kakizoe[1]

[1]Urology Division, National Cancer Center Hospital; [2]Pathology Division, National Cancer Center Research Institute, Tokyo, Japan

(Received April 13, 2009/Revised June 18, 2009/Accepted June 22, 2009/Online publication July 30, 2009)

Prostate cancer mass screening using serum prostate-specific antigen (PSA) has been conducted widely in the world. However, little is known about the true prevalence of prostate cancer in the 'normal' PSA range (4.0 ng/mL or less). The aim of the present study was to elucidate the clinicopathological features of prostate cancer occurring in men with a wide range of PSA levels. The study comprised 349 male patients who underwent radical cystoprostatectomy for bladder cancer. Patients who had had treatment for known prostate cancer were excluded. Tissue specimens were reviewed microscopically. Ninety-one patients (26.1%) were found to have prostate cancer, and 68 (74.7%) of these 91 cancers were considered to be clinically significant. Both increasing patient age and PSA level were significantly correlated with an increased incidence of both all and significant prostate cancers. Sixty-five (21.9%) among 297 patients with PSA < 4.0 ng/mL had prostate cancer, and 45 (69.2%) of the 65 cancers were significant cancers. Eighteen patients had prostate cancers 0.5 mL or more in volume. Among the 18 patients, the PSA level was 4 ng/mL or more in 11, and 3 ng/mL or more in 15. Our study shows that prostate cancer is a common finding in radical cystoprostatectomy specimens excised because of bladder cancers, and a significant proportion of these cancers are clinically significant. PSA still appears to be a useful screening tool for detecting prostate cancers with significant volume. (*Cancer Sci* 2009; 100: 1880–1884)

Prostate cancer is one of the leading causes of mortality and morbidity in developed countries.[1] Screening of serum PSA followed by systematic prostate biopsy has enabled detection of prostate cancer at an earlier stage,[2] although it is still debatable whether mass screening using PSA contributes significantly to reduction in mortality from prostate cancer.[3]

Historically, 4.0 ng/mL PSA has been used as the threshold to prompt prostate biopsy. Although it is known that prostate cancers do exist even in the low PSA range (4.0 ng/mL or less),[4] until recently little was known about the true prevalence of prostate cancer in the low PSA range because most men in this category do not undergo prostate biopsy.[5] In 2004, Thompson *et al.* reported data from the PCPT showing that biopsy-detectable prostate cancer is not rare among men with a low PSA level (4.0 ng/mL or less).[6] This result provoked a discussion about the optimal threshold of PSA for recommending biopsy, although no definitive agreement has been reached so far.[7,8] Although the PCPT demonstrated the prevalence of biopsy-detectable prostate cancer in the low PSA range, there is still a notable lack of data based on thorough histological evaluation of the whole prostate in relation to PSA level in a large general population.

It is possible to microscopically examine the whole prostate of autopsied individuals in whom prostate cancer had not been suspected before death.[9] Although most latent prostate cancers observed in autopsy cases are small lesions, their histology is not different from clinical cancers, and they may be merely in the early phase of progression.[10,11] Usually, however, PSA levels are not available in autopsy cases.

Radical cystoprostatectomy (RCP) is a gold-standard treatment for invasive bladder cancer.[12] Even though some researchers have reported an epidemiological association between bladder cancer and prostate cancer,[13] the specimen obtained from this operation represents a fairly random sample of whole prostate tissue from asymptomatic men. Several studies have examined the incidence and histopathological characteristics of prostate cancer found incidentally in RCP specimens.[14–18] They showed that incidental prostate cancer is not rare in RCP specimens (incidence, 4–60%).[14–18] However, only a few of them examined its relationship with PSA value.[15–18]

In order to elucidate the incidence and histopathological features of prostate cancers occurring in men with a wide range of PSA levels, we reviewed 349 whole prostate tissues in RCP specimens excised because of bladder cancer in Japanese men.

Patients and Methods

Medical records of 354 consecutive men who underwent RCP for bladder cancer at the National Cancer Center Hospital between July 1995 and April 2008 were reviewed retrospectively. The study was approved by the institutional review board.

Three men were excluded from the study because they had undergone pelvic irradiation for bladder cancer before RCP. Two were also excluded because they had been diagnosed as having prostate cancer and treated with androgen ablation and/or radiation therapy before RCP. Thus, 349 men were included in the present study.

A routine pathological examination was conducted on all RCP specimens by sectioning the prostate and bladder every 5 mm. A single pathologist (YK) reviewed the specimens microscopically. Each prostate cancer was staged and graded based on the 2002 International Union Against Cancer (UICC) TNM system[19] and 2005 modified International Society of Urological Pathology (ISUP) Gleason grading system.[20] Tumor volume was calculated using the formula:

$$\text{volume} = (\text{width} \times \text{height} \times \text{length}) \times \pi/6 \times 1.5,$$

in which length is calculated from 0.5 cm multiplied by the number of slices containing tumors and 1.5 is a tissue shrinkage factor.[21]

[3]To whom correspondence should be addressed. E-mail: trnakaga@ncc.go.jp

doi: 10.1111/j.1349-7006.2009.01267.x

Table 1. Status and pathology of prostate biopsy and prostate-specific antigen (PSA) levels before radical cystoprostatectomy (RCP) in the 349 patients

PSA	Prostate biopsy before RCP		
	Yes		No biopsy
	Prostate cancer proved	Benign prostatic tissue	
<4 ng/mL	1	0	296
≥4 ng/mL	3	2	44
Unknown	0	0	3

Table 2. Characteristics of prostate cancers found in radical cystoprostatectomy specimens

Characteristic	Patients	
	n	%
Gleason score		
6 or less	24	26.4
7 (3 + 4)	54	59.3
7 (4 + 3)	9	9.9
8–10	4	4.4
pT stage		
pT2	85	93.4
pT3a	3	3.3
pT3b	1	1.1
pT4	2	2.2
Lymph node status		
pN0	89	97.8
pN1	1	1.1
pN2	1	1.1
Surgical margin status		
Not involved by tumor	87	95.6
Involved by tumor	4	4.4
Perineural invasion		
Negative	69	75.8
Positive	22	24.2

The serum PSA level was determined routinely before RCP at the outpatient clinic. Measurement of PSA levels was carried out using the Delfia-PSA assay (Pharmacia Diagnostics Co., Tokyo, Japan) until September 1997, the Lumipulse PSA assay (Fujirebio, Tokyo, Japan) until July 2004, and the Lumipulse PSA-N assay (Fujirebio) thereafter.

Correlations of clinicopathological parameters between groups were analyzed by Mann–Whitney *U*-test or Kruskal–Wallis test. Differences with *P*-values < 0.05 were considered significant.

Results

The median patient age was 65 years (range, 27–89 years). Preoperative PSA levels were not evaluated in 3 of the 349 men. The median preoperative PSA level was 1.28 ng/mL (range, 0.03–20.603 ng/mL) for the 346 patients.

In 6 of the 349 patients, prostate biopsy had been carried out before RCP. The presence or absence of prostate biopsy, pathology of the biopsy specimen, and serum PSA levels in the 349 patients are summarized in Table 1.

Ninety-one patients (26.1%) were found to have prostate cancer. Of these, four (1.1%) had been preoperatively diagnosed as having prostate cancer by needle biopsy, but had not been treated before RCP. Eighty-seven (24.9%) were found to have incidental prostate cancer.

The pathological features of these 91 prostate cancers are shown in Table 2. The distribution of the prostate cancer volumes

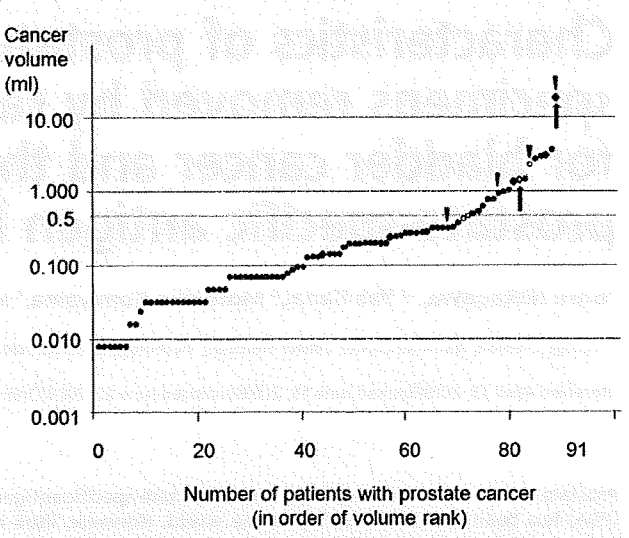

Fig. 1. Volume distribution of prostate cancers. All 91 prostate cancers are plotted in order of volume rank. Each circle and square indicates one prostate cancer. Squares indicate pT3 or pT4 cancers. Clear circles and squares indicate cancers diagnosed by biopsy before cystoprostatectomy. Arrowheads indicate cancers with a Gleason score of 8 or more. Arrows indicate cancers with lymph node metastasis.

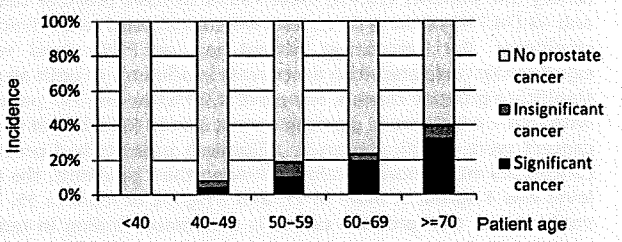

	<40	40–49	50–59	60–69	>=70
Number of patients	6	25	80	128	110
All prostate cancer	0 0%	2 8.0%	15 18.8%	30 23.4%	44 40%
Significant cancer	0 0%	1 4.0%	8 10.0%	24 18.8%	35 31.8%

Fig. 2. Incidence of prostate cancer in each age group. The definition of significant cancer is given in the Results section.

is shown in Figure 1. Larger cancers were more likely to have a higher Gleason score and to have lymph node metastasis (Fig. 1). As for the relationship between cancer volume and pT stage, even small cancers could be at high pT stage: a cancer 0.23 mL in volume showed extracapsular extension (pT3a). A cancer 0.13 mL in volume arose in the prostatic base and invaded to the bladder neck (pT4).

The incidence of prostate cancer increased with patient age (Fig. 2). The median age of the patients with prostate cancer was 69 years (range, 43–81 years), and was significantly higher than that of patients without prostate cancer (median, 63.5 years; range, 27–89 years) ($P < 0.0001$, Mann–Whitney *U*-test).

The incidence of prostate cancer increased with the PSA level (Fig. 3). The median PSA level in the patients with prostate cancer was 1.90 ng/mL (range, 0.26–20.60) and was significantly higher than in those without prostate cancer (median 1.20 ng/mL, range 0.03–13.27 ng/mL) ($P < 0.0001$, Mann–Whitney *U*-test).

Prostate cancer was considered clinically significant if any of the following criteria were present: total tumor volume ≥ 0.5 mL,

Table 3. Relationship between prostate cancer and patient age

Prostate cancer	No. patients	Median age (years)	P-value			
No prostate cancer	258	63.5 (range 27–89)	$P < 0.0001$*			
Prostate cancer	91	69 (range 43–81)		$P = 0.2340$*	$P < 0.0001$†	$P < 0.0001$*
Insignificant	23	67 (range 43–78)				
Significant	68	70 (range 46–81)		$P = 0.1216$*		

*Mann–Whitney *U*-test, †Kruskal–Wallis test.

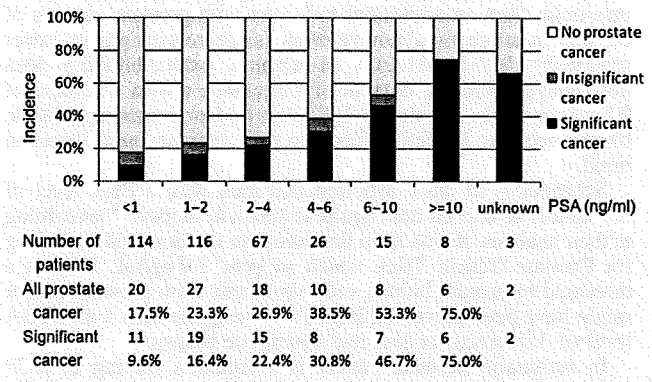

Fig. 3. Incidence of prostate cancer in each prostate-specific antigen (PSA) range. Definition of significant cancer is given in the Results section.

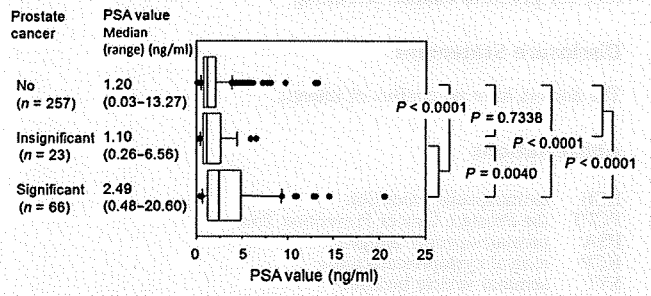

Fig. 4. Relationship between prostate cancer and prostate-specific antigen (PSA) value. The boxes show a range of 25–75 percentiles, and the whiskers a range of 10–90 percentiles. The vertical bars in each box indicate median values. Correlation was calculated using the Mann–Whitney *U*-test.

Gleason grade ≥ 4, ECE, SVI, or lymph node metastasis. Sixty-eight patients (74.7%) had significant prostate cancer. The reasons for designating these cancers as 'significant' were: tumor volume ≥ 0.5 mL in 18 patients (19.8%), Gleason grade ≥ 4 in 67 patients (73.6%), ECE in five patients (5.5%), SVI in one patient (1.1%), and lymph node metastasis in two patients (2.2%).

The incidence of significant prostate cancer increased with patient age (Fig. 2). The median age of the patients with significant prostate cancer was 70 years (range, 46–81 years), and was significantly higher than that of patients without significant prostate cancer (median, 64 years; range, 27–89 years) ($P < 0.0001$, Mann–Whitney *U*-test) (Table 3).

The incidence of significant prostate cancer increased with the PSA level (Fig. 3). Figure 4 shows the distribution of PSA levels in the patients with significant, insignificant, or no prostate cancer. The median PSA level in the patients with significant prostate cancer was 2.49 ng/mL (range, 0.48–20.60 years) and was significantly higher than in those with insignificant cancer (median, 1.10 ng/mL; range, 0.26–6.56 ng/mL) ($P = 0.0040$) and in those without cancer (median, 1.20 ng/mL; range 0.03–13.27 ng/mL) ($P < 0.0001$). The PSA level in the patients with insignificant prostate cancer was not significantly different from that in patients without cancer ($P = 0.7338$) (Fig. 4).

The median follow-up period was 36 months (range, 1–128 months) for the 91 patients with prostate cancer. None of the patients died of prostate cancer during follow-up. One patient, who had a preoperative PSA level of 5.0 ng/mL and a Gleason grade 4 + 3 prostate cancer 2.96 mL in volume, developed biochemical recurrence (PSA recurrence; PSA > 0.2 ng/mL) at 36 months after surgery without any detectable mass lesion. His serum PSA level was 0.583 ng/mL, and no additional therapy has yet been started at 42 months of follow-up.

Discussion

The incidence of prostate cancer varies among races; East Asians have a lower cumulative incidence than white and black people in the USA and Europe.[22] However, the incidence of latent prostate cancer does not differ between Japanese and white and black people in the USA.[9] Latent cancer is not different from clinical cancer in terms of histology.[10,11] The proportion of Japanese men who undergo PSA screening remains at only 5%,[23] whereas 75% of men aged 50 years or older have had a PSA test in the USA.[24] In Japan, however, the morbidity and mortality of prostate cancer have been increasing,[22] and its incidence will increase further as more men undergo PSA mass screening. Our study shows that the incidence of prostate cancer in RCP specimens from Japanese men is consistent with previous reports from the USA and Western Europe,[14–18] and similar to the reported incidences (22.5–34.6%) in Japanese autopsy cases.[9]

With regard to the age distribution of prostate cancer, Ashley showed that there is a linear relationship between the frequency of prostate cancer and age when plotted double logarithmically, and that its slope is 3.[25] In other words, the age-specific incidence of prostate cancer increases approximately with the third power of age.[25] Our present data are consistent with Ashley's classic paper (Fig. 5). Although Ashley considered that the development of prostate cancer requires three (epi)genetic events, based on the Armitage and Doll multistage carcinogenesis model,[26] our data should not be interpreted so simply; the number of (epi)genetic events required for prostate carcinogenesis cannot be determined solely on the basis of incidence data. However, we were able to confirm that prostate carcinogenesis is highly age dependent. Moreover, when we plotted the incidence of significant cancer on the same graph, the plot was linear with a slope of 4 (Fig. 5), indicating that progression to significant prostate cancer requires additional (epi)genetic events.

The PCPT revealed that a considerable proportion of men with low PSA values have prostate cancer.[6] Consequently, it has been suggested that the 'normal' PSA threshold should be discarded.[8] Moreover, there has been an argument that the significance of PSA as a tumor marker has been lost, and that PSA is better regarded as a marker of benign prostatic hyperplasia.[27] Thus, the significance of PSA in screening and prognostication

doi: 10.1111/j.1349-7006.2009.01267.x

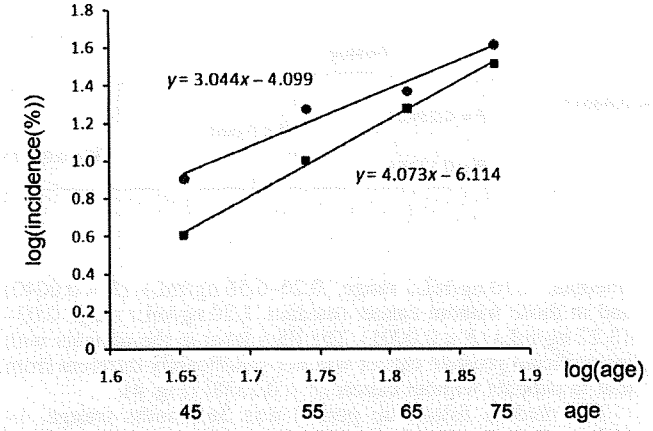

Fig. 5. Incidence of all (circles) and significant (squares) prostate cancers in every decade of patient age presented as a double logarithmic graph. Approximate lines are shown.

has recently been questioned. However, our present study indicates that increasing PSA levels are certainly associated with a higher incidence of all and significant prostate cancers. For example, the incidence of prostate cancer in patients with a PSA level ≥3 ng/mL (35/74, 47.3%) was significantly higher than in patients with a PSA level <3 ng/mL PSA (54/272, 19.9%) ($P < 0.0001$, χ^2-test). Thus, our data suggest that PSA would still be a useful screening tool for prostate cancer, at least in Japan where PSA screening is less prevalent than in Western countries.

In our study 73.5% of 'significant' cancers were small (less than 0.5 mL). Haas *et al.* reported that only 11% of cancers with a volume of less than 0.5 mL, which was estimated by computerized planimetry using an image analysis program, were detectable by 12-core biopsy in autopsy cases.[28] Therefore, most of the small 'significant' cancers in the present study would not have been detectable with current biopsy techniques. However, it is unlikely that all of these small 'significant' cancers need to be detected at such an early stage: McNeal reported that the probability of metastasis is correlated with cancer volume and grade.[11] In our present cohort of prostate cancers, we observed that most cancers with a Gleason score of ≥8 or with nodal metastasis had a volume of 0.5 mL or more (Fig. 1). Overlooking small 'significant' cancers would not compromise prognosis if patients were undergoing periodic PSA screening.

Eighteen of our patients had prostate cancers of 0.5 mL or more, which corresponds to a tumor approximately 1.0 cm in diameter. If PSA = 3.0 ng/mL were used as a threshold for recommending prostate biopsy, then 15 men with prostate cancers of 0.5 mL or more would have been included (sensitivity, 15/18 = 83.3%; specificity, 269/328 = 82.0%; positive predictive value, 15/74 = 20.3%). If PSA = 4.0 ng/mL were applied as a threshold, then an additional four men with prostate cancers of 0.5 mL or more would have been missed, resulting in lower sensitivity (11/18 = 61.1%). In addition, prostate biopsy does not always guarantee detection of all cancers with a volume of 0.5 mL or more. The threshold PSA level for prompting prostate biopsy needs to be determined carefully bearing these issues in mind.

Schröder *et al.* have reported that men with a PSA level of 3.0 ng/mL or less do not require immediate biopsy:[29] according to their analysis of data from the European Randomized Screening for Prostate Cancer Trial, which adopted 3.0 ng/mL PSA as a threshold to prompt biopsy, only six deaths from prostate cancer might have been prevented if all 15 773 eligible men with a PSA level of 3.0 ng/mL or less had undergone biopsy.

In summary, prostate cancer is a common finding in RCP specimens, with a significant proportion having the characteristics of clinically significant prostate cancer. Increasing patient age and PSA value are associated with a high incidence of all and significant prostate cancers, and PSA still appears to be a useful tool for prostate cancer screening

Disclosure Statement

The authors have no conflict of interest.

Abbreviations

ECE	extracapsular extension
PCPT	the Prostate Cancer Prevention Trial
PSA	prostate-specific antigen
RCP	radical cystoprostatectomy
SVI	seminal vesicle invasion

References

1 Jemal A, Siegel R, Ward E *et al.* Cancer statistics, 2008. *CA Cancer J Clin* 2008; **58**: 71–96.
2 Catalona WJ, Smith DS, Ratliff TL *et al.* Measurement of prostate-specific antigen in serum as a screening test for prostate cancer. *N Engl J Med* 1991; **324**: 1156–61.
3 Crawford ED, Thompson IM. Controversies regarding screening for prostate cancer. *BJU Int* 2007; **100**(Suppl 2): 5–7.
4 Catalona WJ, Smith DS, Ornstein DK. Prostate cancer detection in men with serum PSA concentrations of 2.6 to 4.0 ng/mL and benign prostate examination. Enhancement of specificity with free PSA measurements. *JAMA* 1997; **277**: 1452–5.
5 Punglia RS, D'Amico AV, Catalona WJ, Roehl KA, Kuntz KM. Effect of verification bias on screening for prostate cancer by measurement of prostate-specific antigen. *N Engl J Med* 2003; **349**: 335–42.
6 Thompson IM, Pauler DK, Goodman PJ *et al.* Prevalence of prostate cancer among men with a prostate-specific antigen level < or = 4.0 ng per milliliter. *N Engl J Med* 2004; **350**: 2239–46.
7 Welch HG, Schwartz LM, Woloshin S. Prostate-specific antigen levels in the United States: implications of various definitions for abnormal. *J Natl Cancer Inst* 2005; **97**: 1132–7.
8 Thompson IM, Ankerst DP, Etzioni R, Wang T. It's time to abandon an upper limit of normal for prostate specific antigen: assessing the risk of prostate cancer. *J Urol* 2008; **180**: 1219–22.
9 Yatani R, Shiraishi T, Nakakuki K *et al.* Trends in frequency of latent prostate carcinoma in Japan from 1965–79 to 1982–86. *J Natl Cancer Inst* 1988; **80**: 683–7.
10 Stamey TA, Freiha FS, McNeal JE, Redwine EA, Whittemore AS, Schmid HP. Localized prostate cancer. Relationship of tumor volume to clinical significance for treatment of prostate cancer. *Cancer* 1993; **71**(Suppl 3): 933–8.
11 McNeal JE. Prostatic microcarcinomas in relation to cancer origin and the evolution to clinical cancer. *Cancer* 1993; **71**(Suppl 3): 984–91.
12 Stein JP, Skinner DG. Radical cystectomy for invasive bladder cancer: long-term results of a standard procedure. *World J Urol* 2006; **24**: 296–304.
13 Kurokawa K, Ito K, Yamamoto T *et al.* Comparative study on the prevalence of clinically detectable prostate cancer in patients with and without bladder cancer. *Urology* 2004; **63**: 268–72.
14 Damiano R, Di Lorenzo G, Cantiello F *et al.* Clinicopathologic features of prostate adenocarcinoma incidentally discovered at the time of radical cystectomy: an evidence-based analysis. *Eur Urol* 2007; **52**: 648–57.
15 Hautmann SH, Conrad S, Henke RP *et al.* Detection rate of histologically insignificant prostate cancer with systematic sextant biopsies and fine needle aspiration cytology. *J Urol* 2000; **163**: 1734–8.
16 Ward JF, Bartsch G, Sebo TJ, Pinggera GM, Blute ML, Zincke H. Pathologic characterization of prostate cancers with a very low serum prostate specific antigen (0–2 ng/mL) incidental to cystoprostatectomy: is PSA a useful indicator of clinical significance? *Urol Oncol* 2004; **22**: 40–7.
17 Winkler MH, Livni N, Mannion EM, Hrouda D, Christmas T. Characteristics of incidental prostatic adenocarcinoma in contemporary radical cystoprostatectomy specimens. *BJU Int* 2007; **99**: 554–8.

18 Thomas C, Wiesner C, Melchior S, Gillitzer R, Schmidt F, Thüroff JW. Indications for preoperative prostate biopsy in patients undergoing radical cystoprostatectomy for bladder cancer. *J Urol* 2008; **180**: 1938–41.
19 Sobin LH, Fleming ID. *TNM Classification of Malignant Tumors*, 6th edn. Union Internationale Contre le Cancer and the American Joint Committee on Cancer, 2002.
20 Epstein JI, Allsbrook WC Jr, Amin MB, Egevad LL, ISUP Grading Committee. The International Society of Urological Pathology (ISUP) consensus conference on Gleason grading of prostatic carcinoma. *Am J Surg Pathol* 2005; **29**: 1228–42.
21 Noguchi M, Stamey TA, McNeal JE, Yemoto CE. Assessment of morphometric measurements of prostate carcinoma volume. *Cancer* 2000; **89**: 1056–64.
22 Marugame T, Mizuno S. Comparison of prostate cancer mortality in five countries: France, Italy, Japan, UK and USA from the WHO mortality database (1960–2000). *Jpn J Clin Oncol* 2005; **35**: 690–1.
23 Ito K, Yamamoto T, Takechi H, Suzuki K. Impact of exposure rate of PSA-screening on clinical stage of prostate cancer in Japan. *J Urol* 2006; **175**(Suppl): 477–8.
24 Sirovich BE, Schwartz LM, Woloshin S. Screening men for prostate and colorectal cancer in the United States: does practice reflect the evidence? *JAMA* 2003; **289**: 1414–20.
25 Ashley DJ. On the incidence of carcinoma of the prostate. *J Pathol Bacteriol* 1965; **90**: 217–24.
26 Armitage P, Doll R. The age distribution of cancer and a multi-stage theory of carcinogenesis. *Br J Cancer* 1954; **8**: 1–12.
27 Stamey TA, Caldwell M, McNeal JE, Nolley R, Hemenez M, Downs J. The prostate specific antigen era in the United States is over for prostate cancer: what happened in the last 20 years? *J Urol* 2004; **172**: 1297–301.
28 Haas GP, Delongchamps NB, Jones RF *et al*. Needle biopsies on autopsy prostates: sensitivity of cancer detection based on true prevalence. *J Natl Cancer Inst* 2007; **99**: 1484–9.
29 Schröder FH, Bangma CH, Roobol MJ. Is it necessary to detect all prostate cancers in men with serum PSA levels <3.0 ng/mL? A comparison of biopsy results of PCPT and outcome-related information from ERSPC. *Eur Urol* 2008; **53**: 901–8.

doi: 10.1111/j.1349-7006.2009.01267.x

Cancer Science
The official journal of the Japanese Cancer Association JCA

Quantitative proteomics using formalin-fixed paraffin-embedded tissues of oral squamous cell carcinoma

Ayako Negishi,[1,3] Mari Masuda,[1] Masaya Ono,[1] Kazufumi Honda,[1] Miki Shitashige,[1] Reiko Satow,[1] Tomohiro Sakuma,[6] Hideya Kuwabara,[6] Yukihiro Nakanishi,[2] Yae Kanai,[2] Ken Omura,[3,4,5] Setsuo Hirohashi[1] and Tesshi Yamada[1,7]

[1]Chemotherapy Division and [2]Pathology Division, National Cancer Center Research Institute, Chuo-ku, Tokyo; [3]Oral and Maxillofacial Surgery, [4]Department of Advanced Molecular Diagnosis and Maxillofacial Surgery, Hard Tissue Genome Research Center, and [5]Global Center of Excellence Program, International Research Center for Molecular Science in Tooth and Bone Diseases, Tokyo Medical and Dental University, Bunkyo-ku, Tokyo; Department of Surgery, [6]BioBusiness Group, Mitsui Knowledge Industry, Minato-ku, Tokyo, Japan

(Received April 2, 2009/Revised May 12, 2009/Accepted May 13, 2009/Online publication June 11, 2009)

Clinical proteomics using a large archive of formalin-fixed paraffin-embedded (FFPE) tissue blocks has long been a challenge. Recently, a method for extracting proteins from FFPE tissue in the form of tryptic peptides was developed. Here we report the application of a highly sensitive mass spectrometry (MS)-based quantitative proteome method to a small amount of samples obtained by laser microdissection from FFPE tissues. Cancerous and adjacent normal epithelia were microdissected from FFPE tissue blocks of 10 squamous cell carcinomas of the tongue. Proteins were extracted in the form of tryptic peptides and analyzed by 2-dimensional image-converted analysis of liquid chromatography and mass spectrometry (2DICAL), a label-free quantitative proteomics method developed in our laboratory. From a total of 25 018 peaks we selected 72 mass peaks whose expression differed significantly between cancer and normal tissues ($P < 0.001$, paired *t*-test). The expression of transglutaminase 3 (TGM3) was significantly down-regulated in cancer and correlated with loss of histological differentiation. Hypermethylation of *TGM3* gene CpG islands was observed in 12 oral squamous cell carcinoma (OSCC) cell lines with reduced TGM3 expression. These results suggest that epigenetic silencing of TGM3 plays certain roles in the process of oral carcinogenesis. The method for quantitative proteomic analysis of FFPE tissue described here offers new opportunities to identify disease-specific biomarkers and therapeutic targets using widely available archival samples with corresponding detailed pathological and clinical records. (*Cancer Sci* 2009; 100: 1605–1611)

Squamous cell carcinoma is the major histological type of oral cancer and develops in various anatomical locations within the oral cavity, including the tongue, bucca, oropharynx, gingiva, palate, lip, and floor of the mouth. Despite recent improvements in surgical techniques and chemo/radiotherapy,[1] the overall 5-year survival rate for patients with oral squamous cell carcinoma (OSCC) is still unsatisfactory.[2] OSCC has a propensity for rapid local invasion and spread[3] and is considered to be one of the most aggressive forms of squamous cell carcinoma of the head and neck region. Furthermore, the incidence of OSCC has been increasing among the young and middle-aged.[4–6] Therefore, there is an urgent need to develop new diagnostic and therapeutic modalities to improve the outcome of OSCC. Although there is considerable epidemiological evidence for a significant association of alcohol consumption, tobacco smoking, chronic mechanical stimulation, and betel quid chewing with the incidence of OSCC, the molecular mechanisms responsible for OSCC have not been fully elucidated. Overall gene expression in OSCC has been studied extensively over the past decade using microarray techniques. However, gene expression is not always correlated with the expression levels of the corresponding proteins.[7] Although it is anticipated that protein expression reflects more directly the biological and pathological status of diseases, aberrations of protein expression during the course of oral carcinogenesis are largely unknown.

Although the use of fresh material is desirable for any analytical technology, human tissue samples are not always available in sufficient quantity. Formalin-fixed paraffin-embedded (FFPE) tissue blocks are routinely preserved and stored after pathological diagnosis, and such archived material may provide an ample alternative resource for research purposes. However, FFPE specimens have usually not been used for proteomic analyses, as formaldehyde-induced intermolecular and intramolecular cross-linking hinders the solubility of proteins and complicates the extraction of intact proteins from the samples.[8] Recently, a method of extracting proteins from FFPE tissues in the form of tryptic peptides was developed, and the methodology is compatible with a variety of subsequent mass spectrometry (MS)-based proteome applications.[9,10]

We previously developed a MS-based quantitative proteome platform named 2DICAL (2-dimensional image converted analysis of liquid chromatography and mass spectrometry)[11] for quantitative comparison of large peptide datasets generated by nano-flow liquid chromatography and mass spectrometry (LC-MS). Owing to its simple procedure, 2DICAL is highly sensitive and reproducible: 60 000–160 000 peptides can be readily detected in a 1-h LC run and accurately quantified without isotope labeling. In the present study we used 2DICAL for quantitative analysis of small samples of protein obtained from FFPE tissues by laser microdissection and searched for proteins that were differentially expressed between normal and cancerous epithelia of the oral cavity. Here we report the identification of transglutaminase 3 (*TGM3*) as an epigenetically silenced gene in OSCC cell lines.

Materials and Methods

Clinical samples and cell lines. FFPE tissues ($n = 63$) were collected from OSCC patients who underwent surgery at two medical institutions: the National Cancer Center Hospital (NCCH; Tokyo, Japan) between April 1997 and March 2006, and the Tokyo Medical and Dental University Hospital (TMDUH; Tokyo, Japan) between January 2001 and December 2006. All the patients were preoperatively diagnosed as having squamous cell carcinoma of the tongue. Surgically removed tongue tissues were routinely processed for pathological examination, fixed in formalin, embedded in paraffin,

[7]To whom correspondence should be addressed. E-mail: tyamada@ncc.go.jp

doi: 10.1111/j.1349-7006.2009.01227.x

and stored at room temperature. Pathological examination confirmed the histology of invasive squamous cell carcinoma. None of the patients had received preoperative radiation, chemotherapy, or immunotherapy. The cases were followed up for at least 3 years after surgery. Fresh oral mucosa was donated by a volunteer who had no history of malignancy. The protocol of the study was reviewed and approved by the ethics committee boards of the NCC and TMDU.

Twelve OSCC cell lines (Ca9-22, Ho-1-N-1, Ho-1-u-1, HSC-2, HSC-3, HSC-4, HSC-6, KON, KSOC-2, KSOC-3, SAS, SKN-3) were obtained from the Japan Health Science Foundation (Osaka, Japan) and cultured in Dulbecco's modified Eagle medium supplemented with 10% fetal bovine serum.

A plasmid expressing TGM3 (namely pcDNA3.1/TGM3) was constructed by cloning the full-length coding sequence of TGM3 cDNA into the pcDNA3.1 vector (Invitrogen, Carlsbad, CA, USA). pcDNA3.1/TGM3 or the control empty vector (pcDNA3.1) was transfected into cells using the Lipofectamine LTX reagent (Invitrogen).

Laser microdissection and peptide extraction. Paired tumor and adjacent normal epithelial cells were collected from the same FFPE tissues of the NCCH cases ($n = 10$). To recover cell populations of interest without contamination, we used laser microdissection. Ten-micrometer-thick FFPE sections were placed on DIRECTOR Laser Microdissection Slides (Expression Pathology, Gaithersburg, MD, USA), deparaffinized, and stained with hematoxylin–eosin (HE). Parts of the sections 3 mm^2 in area (corresponding to approximately 10 000 cells) were then microdissected using a LMD6000 (Leica Microsystems, Wetzlar, Germany). Proteins were extracted in the form of tryptic peptides utilizing a Liquid Tissue MS Protein Partitioning Kit (Expression Pathology) in accordance with the manufacturer's protocol. In brief, the microdissected tissues were suspended in Liquid Tissue buffer, incubated at 95°C for 90 min, and then cooled on ice for 3 min. Trypsin (15–18 units) was added, and the samples were incubated at 37°C overnight. Dithiothreitol was added to a final concentration of 10 mM, and the samples were heated for 5 min at 95°C. The extracted peptide samples were stored at –80°C until analysis.

Liquid chromatography and mass spectrometry (LC-MS). Twenty tissue samples (10 paired cancer and normal tissues) were blinded, randomized, and measured in triplicate with a linear gradient of 0–80% acetonitrile in 0.1% formic acid at a speed of 200 nL/min for 60 min using a nano-flow high-performance liquid chromatograph (HPLC) (NanoFrontier nLC; Hitachi High-technologies, Tokyo, Japan) connected to an electrospray ionization quadrupole time-of-flight (ESI-Q-TOF) mass spectrometer (NanoFrontier LD, Hitachi High-technologies) every second in the 400–1600 mass-to-charge ratio (m/z) range. MS peaks were detected, normalized, and quantified using in-house 2DICAL software, as described previously.[11] A serial identification (ID) number was applied to each detected MS peak, from ID1 to ID25018.

Protein identification by tandem mass spectrometry (MS/MS). MS/MS spectra were acquired from preparative LC. LC-MS data were aligned with a tolerance of ±0.5 m/z and a retention time (RT) of ±0.4 min, and targeted MS/MS was performed. Peak lists were generated using the MassNavigator software package (Version 1.2; Mitsui Knowledge Industry, Tokyo, Japan) and searched against the NCBInr database (NCBInr_20070419.fast) using the Mascot software package (Version 2.2.1; Matrix Sciences, London, UK). Initial peptide tolerances in MS and MS/MS modes were ±0.05 Da and ±0.1 Da, respectively. Trypsin was designated as the enzyme, and up to one missed cleavage was allowed. The score threshold to achieve $P < 0.05$ is set by the Mascot algorithm, based on the size of the database used in the search.

Immunohistochemistry (IHC). FFPE sections of NCCH ($n = 10$) and TMDUH ($n = 53$) cases were used for IHC. Immunoperoxidase staining was performed using the avidin–biotin–proxidase complex method as described previously.[12,13] Mouse monoclonal anti-TGM3 (1:150; Abnova, Taipei, Taiwan), anti-cytokeratin 4 (CK4) (1:200; Chemicon, Rosemont, IL, USA), anti-cytokeratin 13 (CK13) (1:200; Abcam, Cambridge, UK), and anti-annexin A1 (ANXA1) (1:200; BD Bioscience, Pharmingen, NJ, USA) antibodies and relevant secondary biotin-conjugated antibodies (1:200; Vector Laboratories, Peterborough, UK) were used. Two investigators (K.H., A.N.) blinded to the clinical data reviewed the stained sections. Normal tongue epithelium in the same section served as an internal positive control. Cases in which 10% or more of the tumor cells were positively stained with anti-TGM3 antibody were considered to be TGM3-positive, while cases in which less than 10% of the tumor cells were TGM3-positive were considered to be TGM3-negative. If considerable tumor heterogeneity was present, staining was evaluated in the predominantly differentiated area of the tumor.

Immunoblot analysis. Cells were washed with phosphate-buffered saline and lyzed in cell lysis buffer (50 mM Tris-HCl pH 7.5, 1% Triton-X100, 150 mM NaCl, 20 mM EDTA). The cell lysates were analyzed by immunoblotting, as described previously,[13] using anti-TGM3 (Abcam), CK14 (Thermo Scientific, Waltham, MA, USA), anti-involucrin (Thermo Scientific), and anti-β-actin (Sigma, St Louis, MO, USA) antibodies.

Cytosine methylation analysis. The detection of CpG islands and design of PCR primers for amplification were performed by Methyl Primer Express Software v1.0 (Applied Biosystems, Foster City, CA, USA). Genomic DNA was extracted using DNeasy Blood and Tissue kits (Qiagen, Valencia, CA, USA). Bisulfite conversion was carried out using 2 μg of genomic DNA and the reagents provided in EpiTect Bisulfite Kit (Qiagen). The converted DNA was subjected to PCR using primer sets (5′-GTTTAAATAAAGG TATTTGGTTTAGAG-3′ and 5′-CTTACCCATACTACTCATACC CAC-3′). The PCR products were visualized by 3% agarose gel electrophoresis and subcloned into the TA vector using a TOPO TA Cloning Kit (Invitrogen). Eight colonies were sequenced using an ABI 3130 (Applied Biosystems).

Real-time reverse-transcription PCR. Cells were treated with 0, 2, or 5 μM 5′-aza-2′-deoxycytidine (5Aza-dC) for 5 days. Total RNA was prepared with an RNeasy Mini Kit (Qiagen). DNase-I-treated RNA was random-primed and reverse-transcribed using a High Capacity RNA-to-cDNA Kit (Applied Biosystems). The TaqMan universal PCR master mix and predesigned TaqMan Gene Expression probe and primer sets were purchased from Applied Biosystems. Amplification data measured as an increase in reporter fluorescence were collected using a PRISM 7000 Sequence Detection system (Applied Biosystems). The level of messenger RNA (mRNA) expression relative to the internal control (β-actin) was calculated by the comparative threshold cycle (C_T) method.[14]

Statistical analysis. Differences between subgroups were tested with paired *t*-test. The clinicopathological variables pertaining to the corresponding patients were analyzed for statistical significance by Fisher's exact test. Statistical analyses were performed using an open-source statistical language R (version 2.7.0) with the optional module design package.

Results

Identification of proteins differentially expressed in tongue cancer. Parts corresponding to an area of 3 mm^2 (approximately 10 000 cells) were microdissected from cancerous and adjacent normal epithelia that lacked significant contamination with infiltrating inflammatory cells, stromal cells, muscular components, vascular components, and necrotic cells (Fig. 1a). Then, 20 paired protein samples were prepared from 10 tongue squamous cell carcinoma (TSCC) cases and analyzed for differential protein expression profiles using the 2DICAL proteome platform. A total of 25 018 MS peaks per sample were readily detected and quantified. Linear regression analysis demonstrated excellent linearity with a mean

doi: 10.1111/j.1349-7006.2009.01227.x

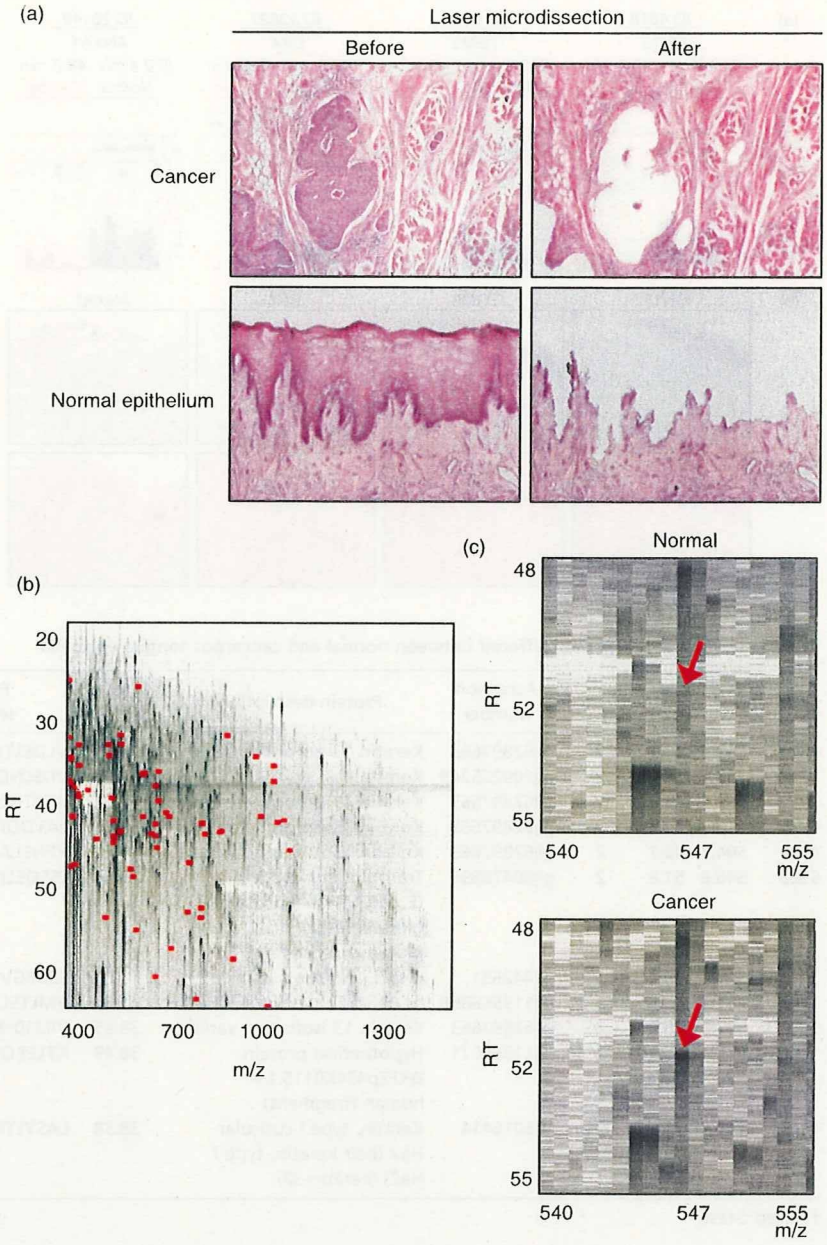

Fig. 1. Identification of proteins differentially expressed in tongue squamous cell carcinoma (TSCC) by 2-dimensional image-converted analysis of liquid chromatography and mass spectrometry (2DICAL). (a) Selective removal of cancerous and normal tongue epithelia from formalin-fixed paraffin-embedded (FFPE) tissues. The microscopic appearances (HE staining) of cancer (top; magnification, ×100) and normal tongue (bottom; magnification, ×40) tissues before (left) and after (right) laser microdissection are shown. (b) Two-dimensional display of all (>25 000) MS peaks of a representative sample with the m/z-values (400–1600 m/z) along the horizontal (*x*) axis and retention time (RT) (20.0–63.0 min) along the vertical (*y*) axis. The 72 MS peaks whose average intensity of triplicates differed significantly between cancer and normal epithelia ($P < 0.001$ [paired *t*-test]) are highlighted in red. (c) Close-up view of a representative MS peak whose intensity differed significantly between normal (top) and cancerous (bottom) epithelia (indicated by red arrows).

correlation coefficient (CC) of 0.9954 (0.9794–0.9989) for the entire 25 018 MS peaks between triplicates (Suppl Fig. S1), confirming the high reproducibility of 2DICAL. The MS peaks detected in a representative run are displayed with m/z along the *x* axis and RT along the *y* axis (Fig. 1b).

Among the total of 25 018 MS peaks, we found 72 whose average intensity of triplicates differed significantly between cancer and normal epithelia as a relatively strict criterion ($P < 0.001$ [paired *t*-test] and average peak intensity >100 [arbitrary unit] for either cancer or control samples) (Fig. 1b, indicated in red; Fig. 1c, indicated by arrows). The intensity of 10 peaks was increased in cancer and that of the remaining 62 peaks was decreased (data not shown). We further selected 12 peaks whose intensity was decreased in cancer by visually inspecting the aligned raw MS spectra (Fig. 2a, top, highlighted in green boxes) and the mean peak intensity (Fig. 2a, bottom) across the 20 samples. A database search using the NCBInr (NCBInr_20070419.fast) for the MS/MS spectra of the 12 peaks identified the amino acid sequences of seven proteins with significant confidence ($P < 0.05$) (Table 1 and Suppl Figs S2–5).

The decreased expression of four proteins, for which antibodies were available, was validated by IHC in 10 TSCC surgical specimens (NCCH) (Fig. 2b). Intense positive immunoreactivity for TGM3, CK13, CK4, and ANXA1 was detected in normal tongue epithelia. Cancerous lesions evidently demonstrated down-regulation of these proteins. ANXA1 staining was observed in all the layers of normal epithelia, whereas only keratinized, but living, cancer cells showed moderate staining for ANXA1 (Fig. 2b). Among these proteins differentially expressed in TSCC, we decided to focus on gaining further insight into the characteristics of TGM3, whose roles in oral carcinogenesis have remained unclear.

Clinicopathological significance of TGM3. To assess the clinical significance of TGM3, its expression was evaluated by IHC in a larger cohort consisting of 53 TSCC cases (TMDUH) (Suppl

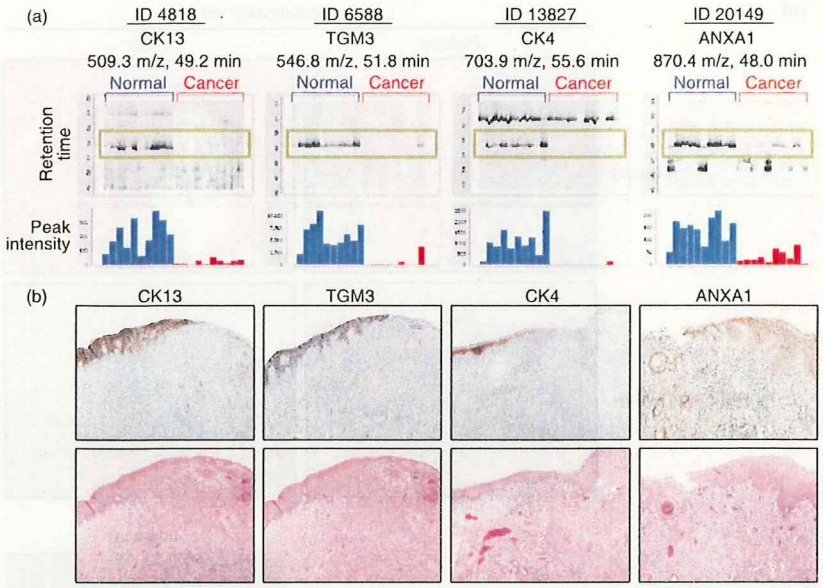

Fig. 2. Identification and validation of differentially expressed proteins. (a) Gel-like views of MS peaks with retention time (RT) along the vertical axes (top) and distribution of the mean peak intensity of triplicates (bottom) across 20 samples (60 liquid chromatography and mass spectrometry [LC-MS] runs). Cancer tissues (red) exhibit reduced expression of the four indicated proteins compared with normal epithelia (blue). (b) Immunoperoxidase staining of CK13, TGM3, CK4, and ANXA1 proteins in tongue squamous cell carcinoma (TSCC) (top) (magnification, ×40). Images of corresponding HE-stained serial sections are shown at the bottom.

Table 1. List of peptides that differed between normal and cancerous tongue epithelia

ID	M/Z	RT	Charge	Accession number	Protein description	Mascot score	Peptide sequence	Normal (mean ± SD)	Cancer (mean ± SD)	*P*-values*
4818	509.3	49.2	2	gi|62897663	Keratin 13 isoform a variant	73.89	VLDELTLSK	6088 ± 2506	491 ± 149	2.56E-04
13 827	703.9	55.6	2	gi|109255249	Keratin 4	59.37	VDSLNDEINFLK	1078 ± 633	23 ± 4	8.76E-04
7777	572.9	44.2	2	gi|62897663	Keratin 13 isoform a variant	54.31	ILTATIENNR	4338 ± 1645	233 ± 82	1.09E-04
673	418.2	47.6	2	gi|62897663	Keratin 13 isoform a variant	53.6	LAVDDFR	9241 ± 3859	848 ± 474	2.51E-04
4572	504.3	46.2	2	gi|62897663	Keratin 13 isoform a variant	47.73	YENELALR	5147 ± 2130	303 ± 95	1.77E-04
6588	546.8	51.8	2	gi|80478896	Transglutaminase 3 (E polypeptide, protein-glutamine-gamma-glutamyltransferase)	42.36	FSSQELILR	209 ± 103	21 ± 15	6.36E-04
20 149	870.4	48.0	2	gi|442631	Chain, annexin I	41.86	SEDFGVNEDLADSDAR	141 ± 51	32 ± 19	5.41E-04
1203	431.3	43.5	2	gi|119568898	hCG1643722, isoform CRA_b	41.57	VMLTELR	9947 ± 4751	561 ± 163	4.78E-04
5504	521.8	48.7	2	gi|62897663	Keratin 13 isoform a variant	38.65	VILEIDNAR	9570 ± 2752	890 ± 302	3.04E-05
12 366	673.4	55.1	2	gi|11360071	Hypothetical protein DKFZp434K0115.1 – human (fragment)	38.49	KTLEEQISEIR	1757 ± 615	73 ± 9	3.40E-05
434	412.3	42.9	2	gi|6016414	Keratin, type I cuticular Ha2 (hair keratin, type I Ha2) (keratin-32)	38.38	LASYLTR	5312 ± 2562	359 ± 91	5.88E-04

†Paired *t*-test.

Fig. S6). In normal tongue mucosa, TGM3 immunoreactivity was confined to the spinous and parakeratinized layers of epithelial cells (Suppl Fig. S6a). Strong nuclear staining for TGM3 was seen in the spinous layer, whereas cytoplasmic staining was detected in the parakeratinized layers. Only 12 out of 53 TSCC cases were positive for TGM3 expression (Table 2). Most cancer cells exhibited sparse immunoreactivity for TGM3 (Suppl Fig. S6c–e) and, when detected, the staining tended to be localized in the differentiated and keratinized area of TSCC (Suppl Fig. S6b). Statistical analysis of the correlation between TGM3 expression and clinicopathologic characteristics demonstrated that TGM3 expression was inversely correlated with loss of histological differentiation ($P < 0.05$, Fisher's exact test), but not with other clinicopathological variables including age, sex, and TNM classification (Table 2).

Lack of TGM3 expression in OSCC cells and its restoration by 5Aza-dC. We next examined TGM3 protein expression in 12 OSCC cell lines by immunoblot analysis. None of these cell lines expressed TGM3 protein. Some of the OSCC cell lines expressed differentiation-associated markers of squamous epithelia, such as CK14 for the proliferative basal layer and involucrin for the upper differentiating layer (Fig. 3a). Real-time PCR analysis to quantify the *TGM3* mRNA expression of these cells gave results consistent with those obtained by immunoblot analysis (data not shown). In an attempt to investigate the molecular mechanism of the gene silencing of *TGM3* in OSCC cells, we grew Ca9-22 cells lacking TGM3 expression in the presence of a methyltransferase inhibitor, 5Aza-dC, for 5 days. Real-time PCR analysis revealed a dose-dependent increase of *TGM3* mRNA expression, and 5-μM 5Aza-dC increased the expression of *TGM3* up to ~60 fold over untreated cells (Fig. 3b). Similar results were obtained in other OSCC cell lines treated with 5Aza-dC (data not shown). Since histone deacetylation, which is catalyzed by the histone deacetylase family, is known to mediate transcriptional repression, we treated Ca9-22 cells with a histone deacetylase inhibitor trichostatin A,

doi: 10.1111/j.1349-7006.2009.01227.x

Table 2. Correlation between clinical characteristics of TSCC and TGM3 protein expression

Characteristics	Total	Number of TGM3-positive cases (%)	Number of TGM3-negative cases (%)	*P*-values*
Total	53	12 (22.6)	41 (77.4)	
Age (years)				
≤60	27	9 (33.3)	18 (66.7)	0.0994
>60	26	3 (11.5)	23 (88.5)	
Gender				
Male	36	8 (22.2)	28 (77.8)	1.0000
Female	17	4 (23.5)	13 (75.5)	
Stage				
I and II	42	10 (23.8)	32 (76.2)	0.4705
III and IV	11	2 (18.2)	9 (81.8)	
TNM classification				
T category				
T1 and T2	48	12 (25.0)	36 (75.0)	0.5765
T3 and T4	5	0 (0)	5 (100)	
N category				
N0	43	12 (27.9)	31 (72.1)	0.0932
N1-3	10	0 (0)	10 (100)	
Histological grade				
Well	22	9 (40.9)	13 (59.1)	0.0171
Moderate or poor	31	3 (9.7)	28 (90.3)	

*P-values were calculated by Fisher's exact test and considered statistically significant at <0.05 (two-sided). TGM3, transglutaminase 3; TSCC, tongue squamous cell carcinoma.

with or without 5Aza-dC. However, this had no effect on the restoration of *TGM3* expression, indicating that histone deacetylation is not responsible for the transcriptional silencing of *TGM3* in OSCC cell lines (data not shown).

Methylation status of the CpG island located in the TGM3 gene upstream region. Reversal of gene silencing of *TGM3* by treatment with 5Aza-dC, but not with TSA, indicated that transcription of the *TGM3* gene was regulated through hypermethylation of the *TGM3* gene promoter and/or enhancer in OSCC cells. A database search of the approximately 20-kb sequence of the human *TGM3* gene including the 5′-flanking region identified a CpG-rich region –6433 to –5958 upstream of the transcription start site (Fig. 3c, top, indicated in a green box). This region was a 475-bp-long fragment containing 22 CpG sites (Fig. 3c, middle, indicated by green vertical bars) and had a GC content of 52.5%, thus meeting the proposed criteria for CpG islands.

To examine the DNA methylation status of these CpG sites in OSCC cells, the entire CpG island was sequenced after bisulfite conversion (Fig. 3c, bottom). All of the 22 CpG sites were recurrently methylated in seven cell lines (Ca9-22, HSC-2, HSC-3, HSC-4, HSC-6, KSOC-3, and SAS). The other five cell lines (Ho-1-N-1, Ho-1-u-1, KON, KSOC-2, and SKN-3) showed patchy methylation of CpG sites 1–4 and 9–16. The entire CpG island in normal oral mucosa was largely unmethylated in five out of eight clones examined. Taken together, these findings suggest that silencing of *TGM3* in OSCC cells is likely attributable to the methylation of CpG sites 5–8 and 19–22.

Discussion

In the present study using our 2DICAL proteome platform, we identified CK4, CK13, TGM3, and ANXA1 as proteins whose expression was significantly decreased in microdissected FFPE tissue samples of TSCC. No protein was up-regulated in TSCC on the basis of the current strict criterion ($P < 0.001$, paired *t*-test), indicating the presence of genetic diversity even within such a small number ($n = 10$) of TSCC samples. IHC analysis of an independent cohort revealed that TGM3 expression was markedly decreased in 41 of 53 (77.4%) TSCC cases and that the reduced expression of TGM3 was clearly correlated with loss of histological differentiation. Consistent with these findings, recent studies utilizing a broad range of genomics and proteomics technologies have begun to reveal the importance of down-regulation of TGM3 in SCC including laryngeal carcinoma,[15] head and neck SCC,[16–21] OSCC developing from leukoplakia,[21] and esophageal SCC.[22,23] Reduction or loss of TGM3 expression in SCC has been reportedly correlated with dedifferentiation,[15,22] an increase in the invasive phenotype,[18] a high incidence of lymph-node metastasis,[20,24] and poor prognosis.[23] Together, these findings strongly implicate a crucial role of TGM3 in oral carcinogenesis.

Transglutaminases (TGMs) are a family of Ca^{2+}-dependent enzymes that catalyze protein cross-linking through formation of intermolecular N^{δ}-(γ-glutamyl) lysine isopeptide linkages.[25–27] TGM3 is a zymogen, requiring activation by proteolytic cleavage, and is expressed predominantly in terminally differentiating stratified squamous epithelium.[26–29] TGM3 is essential for cross-linking cornified cell envelope (CCE) protein constituents and formation of the CCE.[30] To date, nine members of the TGM gene family have been identified in the human genome, including TGM1–7, factor XIII, and erythrocyte band 4.2, a catalytically inactive homolog.[26] Despite marked similarities in the genome structures, their distribution, localization, and mechanism for activation of *TGM* genes are highly variable.[26]

We found that transcription of the *TGM3* gene is regulated by DNA methylation. A database search detected only one CpG island located approximately 6 kb upstream of the transcription start site of the *TGM3* gene. Although the promoter of *TGM3* was reported to be located –126 to –91 bp upstream of the transcripton start site,[28] no CpG island was found in the proximal region. Among 22 CpG sites within the CpG island, methylation of CpG sites 5–8 (region 1) and 19–22 (region 2) was correlated with *TGM3* silencing in the OSCC cell lines, reflecting the possibility that one or both of these two regions function as a distal enhancer for *TGM3* transcription. It is intriguing to note that regions 1 and 2 encompass putative elements for transcription factors including GATA-1 and GATA-2, as well as GATA-1, GATA-2,

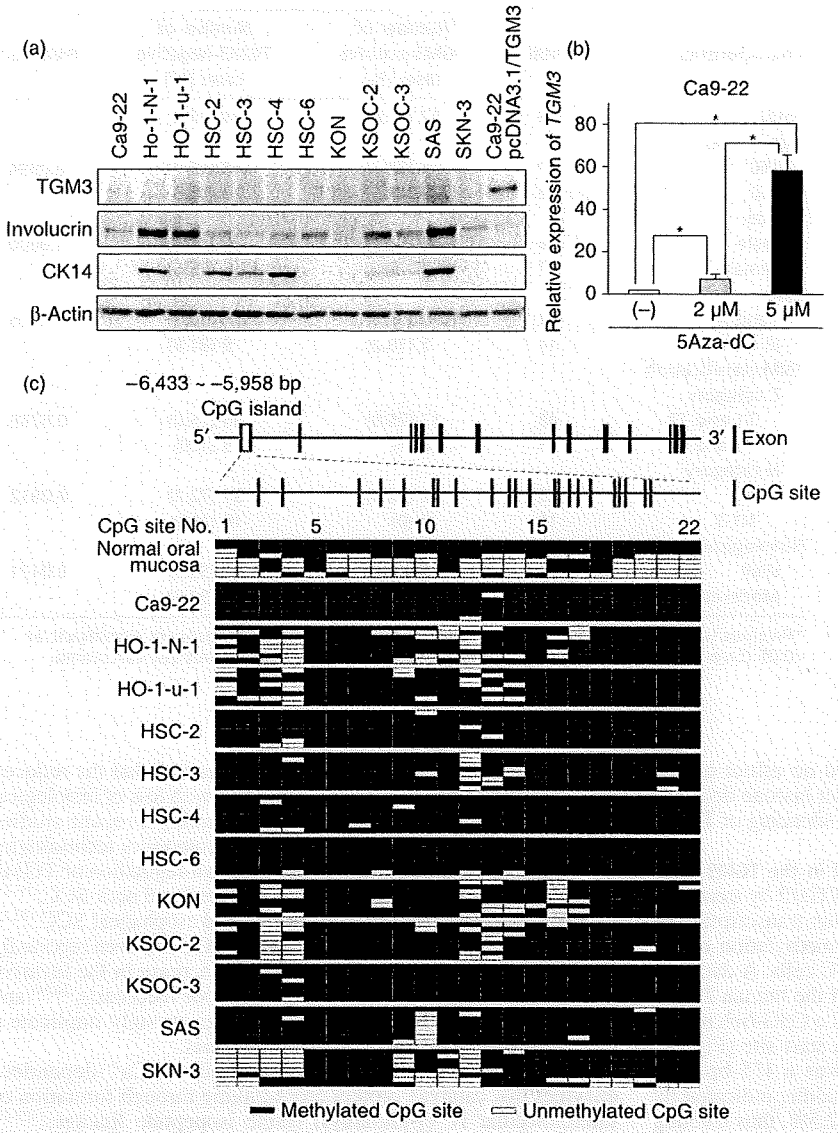

Fig. 3. Epigenetic silencing of transglutaminase 3 (TGM3). (a) TGM3 protein expression in 12 oral squamous cell carcinoma (OSCC) cell lines and Ca9-22 cells transfected with pcDNA3.1/TGM3 (positive control for TGM3). Total cell lysates (10 μg) were analyzed for expression of the indicated proteins by immunoblotting. Involucrin and CK14 were included as epithelial differentiation markers, and β-actin as a loading control. (b) Restoration of TGM3 expression by 5-aza-2′-deoxycytidine (5Aza-dC). Ca9-22 cells were untreated (–) or treated with 2 or 5 μM 5Aza-dC for 5 days. Relative expression levels of the *TMG3* gene were determined by real-time RT-PCR. Columns and bars represent mean ± SD. (c) Cytosine methylation of CpG sites in the upstream region of the *TGM3* gene. Exon/intron structure and the CpG island in the upstream region of the *TGM3* gene are presented schematically (Top). The 22 CpG sites in the CpG island are numbered 1–22 (middle). Genomic DNA was extracted from normal oral mucosa and OSCC cell lines and treated with sodium bisulfite. Eight independent clones per sample were sequenced (bottom). Clear green box, CpG island; vertical blue bars, exons; vertical green bars, CpG sites; clear squares, unmethylated CpG sites; solid squares, methylated CpG sites.

AP-1, and Ets, respectively (www.cbrc.jp/htbin/nph-tfsearch). Transcription factors AP1 and Ets are known to positively regulate epidermal differentiation.[31] It is plausible that tumor-specific hypermethylation in region 2 prevents these transcription factors from binding to their recognition sequences, thereby inactivating transcription of *TGM3*.

Accumulating evidence indicates that TGMs are multifunctional proteins.[26] In fact, some of their functions are even independent of their ability to mediate cross-linking reactions, as exemplified by TGM2, which can function as a molecular switch for transducing cell signaling.[26] TGM2 has been shown to be identical to an atypical high-molecular-weight G-protein known as Ghα, which mediates the activation of phospholipase C through its ability to bind GTP and hydrolyze GTP to GDP.[26,32] Analyses of the crystal structure of TGM3 have indicated that TGM3 possesses a GTP-binding property similar to that of TGM2.[33] TGM3 may also work as a molecular switch governing the cell signaling. *Tgm3* knockout mice show an embryonic-lethal phenotype[34] indicating the non-redundancy of TGM3. This observation also implies that TGM3 has one or more unique functions that cannot be compensated by other TGMs expressed in epithelia, such as TGM1 and TGM5.

Recent advances in proteomic technologies are being increasingly applied to studies of clinical samples in the search for diagnostic biomarkers and therapeutic targets. Here, we have demonstrated for the first time that the powerful combination of the 2DICAL quantitative proteomic high-throughput platform and FFPE archival samples, for which matching clinicopathological information is available, is beginning to show promise.

Acknowledgments

We thank Dr Norihiko Okada (Department of Diagnostic Oral Pathology, Tokyo Medical and Dental University) for advice regarding the design of this study. We also thank Ms Ayako Igarashi, Ms Yuka Nakamura, Ms Satoko Kouda, and Ms Kiyoko Nagumo for their technical assistance. This study was supported by the 'Program for Promotion of Fundamental Studies in Health Sciences' conducted by the National Institute of Biomedical Innovation of Japan, and by the 'Third-Term Comprehensive Control Research for Cancer' and the 'Research on Biological Markers for New Drug Development' conducted by the Ministry of Health, Labor and Welfare of Japan.

Disclosure

None of the authors of this study have a conflict of interest.

doi: 10.1111/j.1349-7006.2009.01227.x

References

1 Forastiere A, Koch W, Trotti A, Sidransky D. Head and neck cancer. *N Engl J Med* 2001; **345**: 1890–900.
2 Spitz MR. Epidemiology and risk factors for head and neck cancer. *Semin Oncol* 1994; **21**: 281–8.
3 Franceschi D, Gupta R, Spiro RH, Shah JP. Improved survival in the treatment of squamous carcinoma of the oral tongue. *Am J Surg* 1993; **166**: 360–5.
4 Mackenzie J, Ah-See K, Thakker N *et al.* Increasing incidence of oral cancer amongst young persons: what is the aetiology? *Oral Oncol* 2000; **36**: 387–9.
5 Annertz K, Anderson H, Biorklund A *et al.* Incidence and survival of squamous cell carcinoma of the tongue in Scandinavia, with special reference to young adults. *Int J Cancer* 2002; **101**: 95–9.
6 Schantz SP, Yu GP. Head and neck cancer incidence trends in young Americans, 1973–97, with a special analysis for tongue cancer. *Arch Otolaryngol Head Neck Surg* 2002; **128**: 268–74.
7 Yamaguchi U, Nakayama R, Honda K *et al.* Distinct gene expression-defined classes of gastrointestinal stromal tumor. *J Clin Oncol* 2008; **26**: 4100–8.
8 Ahram M, Flaig MJ, Gillespie JW *et al.* Evaluation of ethanol-fixed, paraffin-embedded tissues for proteomic applications. *Proteomics* 2003; **3**: 413–21.
9 Patel V, Hood BL, Molinolo AA *et al.* Proteomic analysis of laser-captured paraffin-embedded tissues: a molecular portrait of head and neck cancer progression. *Clin Cancer Res* 2008; **14**: 1002–14.
10 Hwang SI, Thumar J, Lundgren DH *et al.* Direct cancer tissue proteomics: a method to identify candidate cancer biomarkers from formalin-fixed paraffin-embedded archival tissues. *Oncogene* 2007; **26**: 65–76.
11 Ono M, Shitashige M, Honda K *et al.* Label-free quantitative proteomics using large peptide data sets generated by nanoflow liquid chromatography and mass spectrometry. *Mol Cell Proteomics* 2006; **5**: 1338–47.
12 Honda K, Yamada T, Hayashida Y *et al.* Actinin-4 increases cell motility and promotes lymph node metastasis of colorectal cancer. *Gastroenterology* 2005; **128**: 51–62.
13 Shitashige M, Naishiro Y, Idogawa M *et al.* Involvement of splicing factor-1 in β-catenin/T-cell factor-4-mediated gene transactivation and pre-mRNA splicing. *Gastroenterology* 2007; **132**: 1039–54.
14 Huang L, Shitashige M, Satow R *et al.* Functional interaction of DNA topoisomerase IIα with the β-catenin and T-cell factor-4 complex. *Gastroenterology* 2007; **133**: 1569–78.
15 He G, Zhao Z, Fu W, Sun X, Xu Z, Sun K. [Study on the loss of heterozygosity and expression of transglutaminase 3 gene in laryngeal carcinoma]. *Zhonghua Yi Xue Yi Chuan Xue Za Zhi* 2002; **19**: 120–3. (In Chinese.)
16 Gonzalez HE, Gujrati M, Frederick M *et al.* Identification of 9 genes differentially expressed in head and neck squamous cell carcinoma. *Arch Otolaryngol Head Neck Surg* 2003; **129**: 754–9.
17 Choi P, Jordan CD, Mendez E *et al.* Examination of oral cancer biomarkers by tissue microarray analysis. *Arch Otolaryngol Head Neck Surg* 2008; **134**: 539–46.
18 Kondoh N, Ishikawa T, Ohkura S *et al.* Gene expression signatures that classify the mode of invasion of primary oral squamous cell carcinomas. *Mol Carcinog* 2008; **47**: 744–56.
19 Ye H, Yu T, Temam S *et al.* Transcriptomic dissection of tongue squamous cell carcinoma. *BMC Genomics* 2008; **9**: 69.
20 Mendez E, Fan W, Choi P *et al.* Tumor-specific genetic expression profile of metastatic oral squamous cell carcinoma. *Head Neck* 2007; **29**: 803–14.
21 Ohkura S, Kondoh N, Hada A *et al.* Differential expression of the keratin-4-13-14-17 and transglutaminase 3 genes during the development of oral squamous cell carcinoma from leukoplakia. *Oral Oncol* 2005; **41**: 607–13.
22 Liu W, Yu ZC, Cao WF, Ding F, Liu ZH. Functional studies of a novel oncogene TGM3 in human esophageal squamous cell carcinoma. *World J Gastroenterol* 2006; **12**: 3929–32.
23 Uemura N, Nakanishi Y, Kato H *et al.* Transglutaminase 3 as a prognostic biomarker in esophageal cancer revealed by proteomics. *Int J Cancer* 2009; **124**: 2106–15.
24 Uchikado Y, Inoue H, Haraguchi N *et al.* Gene expression profiling of lymph node metastasis by oligomicroarray analysis using laser microdissection in esophageal squamous cell carcinoma. *Int J Oncol* 2006; **29**: 1337–47.
25 Griffin M, Casadio R, Bergamini CM. Transglutaminases: nature's biological glues. *Biochem J* 2002; **368**: 377–96.
26 Lorand L, Graham RM. Transglutaminases: crosslinking enzymes with pleiotropic functions. *Nat Rev Mol Cell Biol* 2003; **4**: 140–56.
27 Esposito C, Caputo I. Mammalian transglutaminases. Identification of substrates as a key to physiological function and physiopathological relevance. *FEBS J* 2005; **272**: 615–31.
28 Lee JH, Jang SI, Yang JM, Markova NG, Steinert PM. The proximal promoter of the human transglutaminase 3 gene. Stratified squamous epithelial-specific expression in cultured cells is mediated by binding of Sp1 and ets transcription factors to a proximal promoter element. *J Biol Chem* 1996; **271**: 4561–8.
29 Hitomi K, Horio Y, Ikura K, Yamanishi K, Maki M. Analysis of epidermal-type transglutaminase (TGase 3) expression in mouse tissues and cell lines. *Int J Biochem Cell Biol* 2001; **33**: 491–8.
30 Kim SY, Chung SI, Steinert PM. Highly active soluble processed forms of the transglutaminase 1 enzyme in epidermal keratinocytes. *J Biol Chem* 1995; **270**: 18026–35.
31 Mack JA, Anand S, Maytin EV. Proliferation and cornification during development of the mammalian epidermis. *Birth Defects Res C Embryo Today* 2005; **75**: 314–29.
32 Nakaoka H, Perez DM, Baek KJ *et al.* Gh: a GTP-binding protein with transglutaminase activity and receptor signaling function. *Science* 1994; **264**: 1593–6.
33 Hitomi K, Ikura K, Maki M. GTP, an inhibitor of transglutaminases, is hydrolyzed by tissue-type transglutaminase (TGase 2) but not by epidermal-type transglutaminase (TGase 3). *Biosci Biotechnol Biochem* 2000; **64**: 657–9.
34 Kim SY, Jeitner TM, Steinert PM. Transglutaminases in disease. *Neurochem Int* 2002; **40**: 85–103.

Supporting Information

Additional Supporting Information may be found in the online version of this article:

Fig. S1. Reproducibility of 2-dimensional image-converted analysis of liquid chromatography and mass spectrometry (2DICAL). The horizontal (x) axis represents the distribution of the peak intensities of a liquid chromatography and mass spectrometry (LC-MS) run (run 1), and the vertical (y) axis represents that of another run (run 2) for the same representative tongue squamous cell carcinoma (TSCC) sample. The average correlation coefficient (CC) of all corresponding 25 018 MS peaks between the duplicates was 0.9992. 94.5% (23 642/25 018) of the peaks are plotted within a two-fold difference (blue lines), and 96.4% (24 117/25 018) within a three-fold difference (red lines).

Fig. S2. Labeled tandem mass spectrometry (MS/MS) spectrum and peak list of ID 4818, which matched the sequences of CK13.

Fig. S3. Labeled tandem mass spectrometry (MS/MS) spectrum and peak list of ID 6588, which matched the sequences of transglutaminase 3 (TGM3).

Fig. S4. Labeled tandem mass spectrometry (MS/MS) spectrum and peak list of ID 13827, which matched the sequences of CK4.

Fig. S5. Labeled tandem mass spectrometry (MS/MS) spectrum and peak list of ID 20149, which matched the sequences of ANXA1.

Fig. S6. Expression of transglutaminase 3 (TGM3) in tongue squamous cell carcinoma (TSCC). The expression of TGM3 protein was evaluated by immunohistochemistry in 53 TSCC cases. Representative images of immunohistochemical staining for TGM3 (a–e) and corresponding HE staining (a′–e′) are aligned side by side (magnification, ×100). TGM3 immunoreactivity was localized predominantly in the cytoplasm and nuclei of non-neoplastic tongue epithelial cells (a). TGM3 is detected in keratinized cancer pearls of some well-differentiated TSCCs (b), but TGM3 immunoreactivity is hardly detectable in moderately (d) or poorly (e) differentiated TSCC.

Please note: Wiley-Blackwell are not responsible for the content or functionality of any supporting materials supplied by the authors. Any queries (other than missing material) should be directed to the corresponding author for the article.

Review Article

Genome-wide DNA methylation profiles in precancerous conditions and cancers

Yae Kanai[1]

Pathology Division, National Cancer Center Research Institute, Tokyo, Japan

(Received August 15, 2009/Revised September 25, 2009/Accepted September 27, 2009/Online publication November 4, 2009)

Alterations of DNA methylation, which result in chromosomal instability and silencing of tumor-related genes, are among the most consistent epigenetic changes observed in human cancers. Analysis of tissue specimens has revealed that DNA methylation alterations participate in multistage carcinogenesis, even from the early and precancerous stages, especially in association with chronic inflammation and/or persistent viral infection, such as chronic hepatitis or liver cirrhosis resulting from infection with hepatitis B or C virus. DNA methylation alterations can account for the histological heterogeneity and clinicopathological diversity of human cancers. Overexpression of DNA methyltransferase 1 is not a secondary result of increased cell proliferative activity, but is significantly correlated with accumulation of DNA hypermethylation in CpG islands of tumor-related genes. Alteration of DNA methyltransferase 3b splicing may result in chromosomal instability through DNA hypomethylation in pericentromeric satellite regions. Genome-wide analysis of DNA methylation status has revealed that the DNA methylation profile at the precancerous stage is basically inherited by the corresponding cancers developing in individual patients. DNA methylation status is not simply altered at the precancerous stage; rather, DNA methylation alterations at the precancerous stage may confer vulnerability to further genetic and epigenetic alterations, generate more malignant cancers, and thus determine patient outcome. Therefore, genome-wide DNA methylation profiling may provide optimal indicators for carcinogenetic risk estimation and prognostication, and thus provide an avenue for cancer prevention and therapy on an individual basis. (*Cancer Sci* 2010; 101: 36–45)

DNA methylation, a covalent chemical modification resulting in addition of a methyl group at the carbon five position of the cytosine ring in CpG dinucleotides, is one of the most consistent epigenetic changes observed in human cancers.[1] DNMTs transfer methyl groups from *S*-adenosylmethionine to cytosines.[2] The preference of DNMT1, a major and well-known DNMT, for hemimethylated over unmethylated substrates *in vitro*,[3] and its targeting of replication foci by binding to PCNA,[4,5] are believed to allow copying of the DNA methylation pattern on the parental strand to the newly synthesized daughter DNA strand. Thus, DNMT1 has been recognized as a "maintenance" DNMT,[6] whereas DNMT3a and DNMT3b show *de novo* DNA methylation activity.[7] DNA methylation normally promotes a highly condensed heterochromatin structure associated with deacetylation of histones H3 and H4, loss of histone H3, lysine 4 (H3K4) methylation, and gain of H3K9 and H3K27 methylation.[8] When methyl-CpG-binding proteins, such as MeCP2[9,10] and MBD2,[11] bind to methylated CpG dinucleotide, their transcriptional repression domain recruits a co-repressor complex containing histone deacetylases. However, histone methyltransferases, such as G9A[12] and SUV39H1,[13] are required to recruit DNMTs. DNA methylation is a stable modification inherited throughout consecutive cell divisions, being essential for the normal development and function of adult organs, particularly for X-chromosome inactivation, genome imprinting, silencing of transposons and other parasitic elements, and proper expression of genes.[14]

Reduction of DNMT1 activity in genetically engineered animals alters the number of tumors or the timing of tumor development, suggesting a causal relationship between DNA methylation alterations and tumorigenesis.[15,16] In 1995, when the *RB* and *VHL* genes were the only tumor suppressor genes known to be silenced by DNA methylation, we showed that the E-cadherin tumor suppressor gene is silenced by DNA methylation around the promoter region.[17] The list of tumor-related genes whose expression levels are altered due to DNA hypo- or hypermethylation is increasing.[18–22] Transcriptionally repressive chromatin modifications within the promoters of tumor-related genes silenced by DNA methylation are known to resemble the chromatin modifications of these genes in normal embryonic stem cells, for example, polycomb complex binding and H3K27 methylation.[23] These genes also have an active marker, H3K4 methylation, in normal stem cells, and this bivalent state is converted to a primary active or repressive chromatin conformation after differentiation cues have been received.[23] During carcinogenesis, such modifications may render the genes vulnerable to errors, resulting in aberrant DNA methylation.[24] DNA hypomethylation induces chromosomal instability through decondensation of heterochromatin and enhancement of chromosomal recombination during carcinogenesis.[25] Translational epigenetics have come of age,[26,27] and empirical analysis of DNA methylation status in clinical tissue samples in connection with the clinicopathological diversity of human cancers is assuming increasing importance for the diagnosis, prevention, and therapy of cancers.[28,29]

Alterations of DNA methylation during multistage carcinogenesis

Alterations of DNA methylation at the precancerous stage. DNA methylation alterations play a key role in the early steps of human carcinogenesis. In the 1990s, although LOH on chromosome 16 was frequently detected by classical Southern blotting in HCCs that were poorly differentiated, large in size, and associated with metastasis,[30] only a few of the molecular events occurring in the earlier stage of hepatocarcinogenesis were known. Since DNA methylation alterations may be correlated with chromosomal instability, we examined the DNA methylation status on chromosome 16 using Southern blotting

[1]To whom correspondence should be addressed.
E-mail: ykanai@ncc.go.jp

doi: 10.1111/j.1349-7006.2009.01383.x

with a DNA methylation-sensitive restriction enzyme. DNA methylation alterations at multiple loci on chromosome 16, compared to normal liver tissue samples, were frequently revealed even in samples of non-cancerous liver tissue showing chronic hepatitis or liver cirrhosis,[31,32] which are widely considered to be precancerous conditions,[33] indicating that DNA methylation alterations are a very early event during multistage hepatocarcinogenesis. This was one of the earliest reports of DNA methylation alterations at the precancerous stage.[31]

DNA hypermethylation around the promoter region of the E-cadherin tumor suppressor gene (16q22.1), which encodes a Ca^{2+}-dependent cell-cell adhesion molecule,[34] has been detected even in samples of non-cancerous liver tissue showing chronic hepatitis or cirrhosis.[35] Heterogeneous E-cadherin expression in such non-cancerous liver tissue, which is associated with small focal areas of hepatocytes showing only slight E-cadherin immunoreactivity, might be due, at least partly, to DNA hypermethylation.[35] Reduction of E-cadherin expression due to DNA methylation around the promoter region may participate even in the very early stage of hepatocarcinogenesis through loss of intercellular adhesiveness and destruction of tissue morphology.

Studies of LOH by PCR using microsatellite markers have been reported, using specimens microdissected from precancerous lesions in several organ types. Whether aberrant DNA methylation precedes chromosomal instability during hepatocarcinogenesis was re-examined using microdissected specimens obtained from lobules, pseudo lobules or regenerative nodules in non-cancerous liver tissue from patients with HCCs by bisulfite modification. Although no degree of DNA methylation of any of the examined C-type CpG islands, which are generally methylated in a cancer-specific but not age-dependent manner, was ever detected in normal liver tissue from patients without HCCs, DNA hypermethylation of such islands was frequently found, even in microdissected specimens of non-cancerous liver tissue showing no remarkable histological changes obtained from patients with HCCs in which LOH was never detected.[36] Thus it was confirmed that aberrant DNA methylation is an earlier event preceding chromosomal instability during hepatocarcinogenesis.

As another example of inflammation-associated carcinogenesis, ductal carcinomas of the pancreas frequently develop after chronic damage due to pancreatitis. At least a proportion of peripheral pancreatic ductal epithelia with an inflammatory background may be at the precancerous stage. When the DNA methylation status of the *p14*, *p15*, *p16*, *p73*, *APC*, *hMLH1*, *MGMT*, *BRCA1*, *GSTP1*, *TIMP-3*, *E-cadherin*, and *DAPK-1* genes was examined, the average number of methylated tumor-related genes and the incidence of DNA methylation of at least one gene were increased in peripheral pancreatic ductal epithelia with an inflammatory background and in another precancerous lesion, PanIN, in comparison with normal peripheral pancreatic duct epithelia.[37]

UCs of the urinary bladder, renal pelvis, and ureter are clinically remarkable because of their multicentricity and tendency to recur (Fig. 1a).[38] A possible mechanism for such multiplicity is the "field effect." Even non-cancerous urothelia showing no remarkable histological changes obtained from patients with UCs can be considered precancerous, because they may have been exposed to carcinogens in the urine. When the DNA methylation status of multiple C-type CpG islands was examined, the average number of methylated C-type CpG islands was increased in non-cancerous urothelia showing no remarkable histological changes obtained from patients with UCs, in comparison with normal urothelia obtained from patients without UCs.[39]

Cigarette smoking is another background factor associated with alterations of DNA methylation during multistage carcinogenesis. DNA hypermethylation at the D17S5 locus, where the *HIC (hypermethylated-in-cancer)-1* tumor suppressor gene was identified, is observed even in non-cancerous lung tissue, which may contain progenitor cells for cancers, obtained from patients with non-small-cell lung cancers. The incidence of DNA hypermethylation in non-cancerous lung tissue obtained from patients with non-small-cell lung cancers is significantly correlated with both smoking history and the extent of pulmonary anthracosis, as an index of the cumulative effects of smoking.[40] Thus, DNA methylation alterations are frequently found even at the precancerous stage in various organs, especially in association with chronic inflammation[41,42] and/or persistent infection with viruses[43–45] or other pathogenic microorganisms, and with cigarette smoking.

DNA methyltransferase 1 overexpression and regional DNA hypermethylation. With respect to the molecular backgrounds of DNA methylation alterations,[46] it has been reported that levels of DNMT1 mRNA expression are significantly higher in samples of non-cancerous liver tissue showing chronic hepatitis or cirrhosis than in normal liver tissue, and are even higher in HCCs.[47,48] The incidence of DNMT1 overexpression in HCCs is significantly correlated with poorer tumor differentiation and portal vein involvement.[49] Moreover, the recurrence-free and overall survival rates of patients with HCCs showing DNMT1 overexpression are significantly lower than those of patients with HCCs that do not.[49]

As mentioned above, at least a proportion of peripheral pancreatic ductal epithelia with an inflammatory background may be at the precancerous stage. The incidence of DNMT1 protein expression increases with progression from peripheral pancreatic ductal epithelia with an inflammatory background, to PanIN, to well-differentiated ductal carcinoma, and finally to poorly differentiated ductal carcinoma of the pancreas, in comparison with normal peripheral pancreatic duct epithelia.[50] DNMT1 overexpression in ductal carcinomas of the pancreas is significantly correlated with the extent of invasion to the surrounding tissue, an advanced stage, and poorer patient outcome.[50] The average number of methylated tumor-related genes in microdissected specimens of peripheral pancreatic ductal epithelia with an inflammatory background, PanIN, and ductal carcinoma was significantly correlated with the level of DNMT1 protein expression examined immunohistochemically in precisely microdissected areas.[37]

Expression levels of DNMT1 mRNA and protein are significantly correlated with poorer differentiation and the CIMP, a cancer phenotype characterized by accumulation of DNA methylation of C-type CpG islands,[51,52] in stomach cancers,[53] but no such association has been observed for the expression of DNMT2, DNMT3a, or DNMT3b.[54] Epstein–Barr virus infection in stomach cancers is significantly associated with marked accumulation of DNA methylation of C-type CpG islands and overexpression of DNMT1 protein.[53] *Helicobacter pylori* infection, another etiologic factor for stomach carcinogenesis, has also been reported to strongly promote regional DNA hypermethylation[55] but is not correlated with DNMT1 expression levels.[53]

It is debatable whether increased DNMT1 expression is due to an increase in the proportion of dividing cells or to an acute increase of DNMT1 expression per individual cancer cell. Immunohistochemical examinations have clearly revealed that the incidence of nuclear DNMT1 immunoreactivity is already higher in non-cancerous urothelia showing no remarkable histological changes obtained from patients with UCs, which may already be exposed to carcinogens in the urine but in which the PCNA labeling index had not yet increased, compared to that in normal urothelia from patients without UCs, indicating that

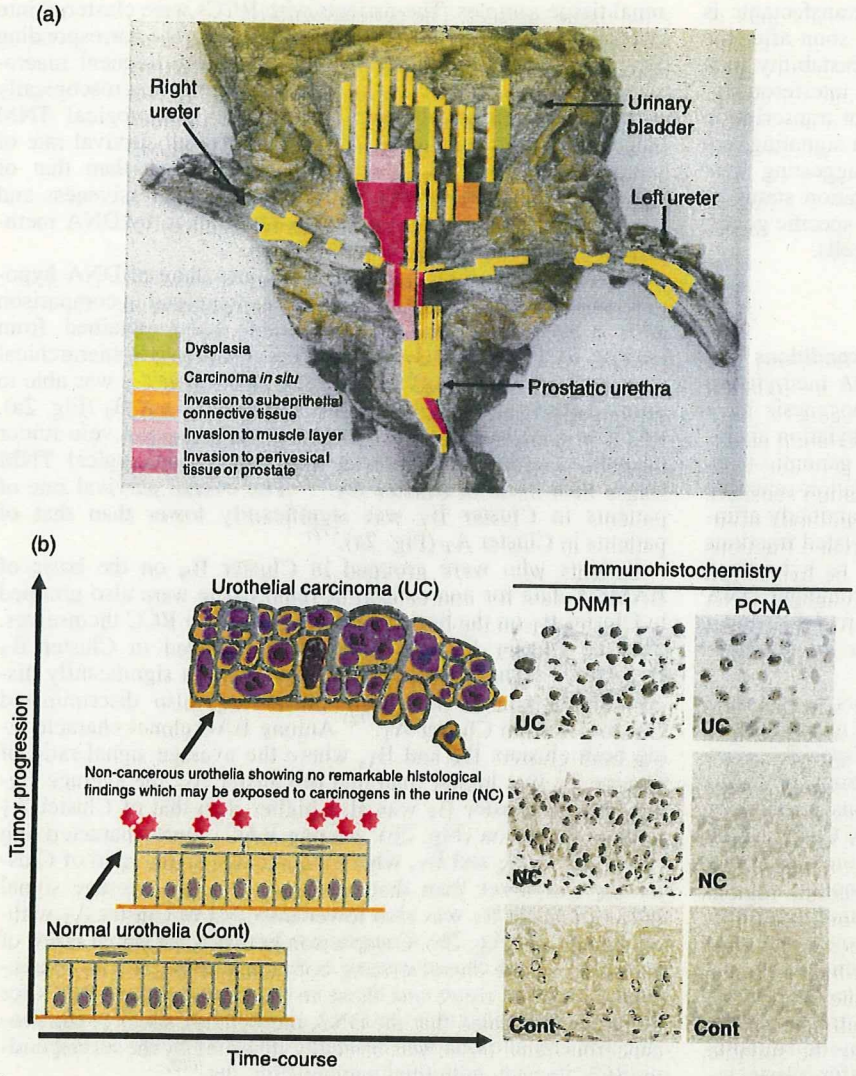

Fig. 1. Overexpression of DNA methyltransferase (DNMT) 1 protein during multistage urothelial carcinogenesis. (a) Specimen obtained by radical cystectomy for multiple urothelial carcinomas (UCs) of the urinary bladder, bilateral ureters, and prostatic urethra. UCs are clinically remarkable because of their multicentricity and tendency to recur: synchronously or metachronously multifocal UCs often develop in individual patients.[38] A possible mechanism for such multiplicity is the "field effect." Even non-cancerous urothelia showing no remarkable histological changes obtained from patients with UCs can be considered precancerous, because they may be exposed to carcinogens in the urine. (b) Immunohistochemical examination for DNMT1 and proliferating cell nuclear antigen (PCNA) in tissue specimens. The incidence of nuclear DNMT1 immunoreactivity had already increased in non-cancerous urothelia showing no remarkable histological changes obtained from patients with UCs (NC), where the PCNA labeling index had not yet increased, compared to that in normal urothelia obtained from patients without UCs (Cont), indicating that DNMT1 overexpression preceded any increase of cell proliferative activity.[56] The intensity of nuclear DNMT1 immunoreactivity was further increased in UCs.[56]

DNMT1 overexpression preceded increased cell proliferative activity (Fig. 1b).[56] The incidence of nuclear DNMT1 immunoreactivity showed a further and progressive increase in dysplastic urothelia, and during transition to UCs (Fig. 1b).[56] Among all examined microdissected specimens of non-cancerous urothelia showing no remarkable histological changes from patients with UCs, or dysplastic urothelia and UCs, accumulation of DNA methylation of C-type CpG islands was significantly correlated with the level of DNMT1 protein expression.[39]

Thus DNMT1 overexpression participates not only in the precancerous stage but also in the malignant progression of various cancers, and has a prognostic impact on patients. DNMT1 overexpression is frequently associated with CIMP of cancers. Although the maintenance activities of DNMT1 are related to its *in vitro* preference for hemimethylated substrates, excessive amounts of DNMT1 in comparison to PCNA may participate in *de novo* methylation of CpG islands. The molecular mechanisms that target DNMT1 to unmethylated substrates in cancers need to be clarified.

Splicing alteration of DNMT3b and DNA hypomethylation in pericentromeric satellite regions. DNA hypomethylation in pericentromeric satellite regions is known to result in centromeric decondensation and enhanced chromosome recombination. In HCCs[57] and UCs,[58] DNA hypomethylation of these regions is correlated with copy number alterations on chromosomes 1 and 9, respectively, where satellite regions are rich. DNMT3b is required for DNA methylation of pericentromeric satellite regions in early mouse embryos, and germline mutations of the *DNMT3b* gene have been reported in patients with immunodeficiency, centromeric instability, and facial anomalies (ICF) syndrome, a rare recessive autosomal disorder characterized by DNA hypomethylation of pericentromeric satellite regions.[59] The major splice variant of DNMT3b in normal liver tissue samples is DNMT3b3, which possesses the conserved catalytic domains.[60] DNMT activity of human DNMT3b3 has been confirmed *in vitro*.[61] In contrast, DNMT3b4 lacks the conserved catalytic domains, although it retains the *N*-terminal domain required for targeting to heterochromatin sites. Samples of normal liver tissue show only a trace level of DNMT3b4 expression.[60] The levels of DNMT3b4 mRNA expression and the ratio of DNMT3b4 mRNA to DNMT3b3 in samples of non-cancerous liver tissue obtained from patients with HCCs, and in HCCs themselves, are significantly correlated with the degree of DNA hypomethylation in pericentromeric satellite regions.[60] DNA demethylation on satellite 2 has been observed in DNMT3b4-transfected human epithelial 293 cells.[60] As DNMT3b4 lacking DNMT activity competes with DNMT3b3 for targeting to pericentromeric satellite regions, DNMT3b4 overexpression may lead to chromosomal instability through induction of DNA hypomethylation in such regions.

doi: 10.1111/j.1349-7006.2009.01383.x

Furthermore, the growth rate of DNMT3b4 transfectants is approximately double that of mock-transfectants soon after the introduction of DNMT3b4, when chromosomal instability may not yet have accumulated.[62] Genes implicated in interferon signaling including signal transducer and activator of transcription (STAT) 1, which acts as an effector of interferon signaling, are upregulated in DNMT3b4 transfectants,[62] suggesting that DNMT3b may act to maintain the DNA methylation status of not only pericentromeric satellite regions but also specific genes, probably in cooperation with DNMT1, in cancer cells.

Genome-wide DNA methylation profiling

DNA methylation profiles in precancerous conditions are inherited by cancers. The above findings that DNA methylation alterations are associated with multistage carcinogenesis have prompted us to carry out genome-wide DNA methylation analysis of tissue specimens. Recently, analysis on a genomic-wide scale has become possible using DNA methylation-sensitive restriction enzyme-based or anti-methyl-cytosine antibody affinity techniques that enrich methylated and unmethylated fractions of genomic DNA.[63,64] These fractions can then be hybridized to DNA microarrays or sequenced. Ultra-high-throughput DNA sequencing technologies are being introduced for the direct sequencing of enriched, methylated fragments or for bisulfite-converted genomic sequencing.[65]

We have used BAMCA.[66–69] Many researchers in this field use the promoter arrays to identify genes that are methylated in cancer cells. However, the promoter regions of specific genes are not the only target of DNA methylation alterations in human cancers. DNA methylation status in genomic regions not directly participating in gene silencing, such as the edges of CpG islands, may be altered at the precancerous stage before the alterations of the promoter regions themselves occur.[70] Genomic regions in which DNA hypomethylation affects chromosomal instability may not be contained in promoter arrays. Moreover, aberrant DNA methylation of large chromosome regions, which are regulated in a coordinated manner in human cancers due to a process of long-range epigenetic silencing, has recently attracted attention.[71] Therefore, we used a BAC array that may be suitable, not for focusing on specific promoter regions, but for overviewing the DNA methylation status of individual large regions among all chromosomes.

When BAMCA methods were applied to samples of non-cancerous renal tissue obtained from patients with clear cell RCCs, many BAC clones showed DNA hypo- or hypermethylation in comparison to normal renal tissue samples from patients without any primary renal tumors.[72] RCCs are usually well demarcated and covered by a fibrous capsule, and hardly ever contain fibrous stroma between cancer cells (Fig. 2a). We were therefore able to obtain cancer cells of high purity from surgical specimens, avoiding contamination with either non-cancerous epithelial cells or stromal cells (Fig. 2a). Therefore, the DNA methylation alterations observed in samples of non-cancerous renal tissue from patients with RCCs cannot be attributable to contamination during sampling. Moreover, DNA methylation alterations in non-cancerous renal tissue did not depend on the distance from the RCC itself to the site from which the non-cancerous renal tissue samples were taken. Because of the lack of any remarkable histological changes or any association with chronic inflammation and persistent infection with viruses or other pathogenic microorganisms, precancerous conditions in the kidney have rarely been described. However, from the viewpoint of DNA methylation, we can consider that non-cancerous renal tissue from patients with RCCs is already at the precancerous stage, showing genome-wide DNA methylation alterations.

We then carried out two-dimensional unsupervised hierarchical clustering analysis based on BAMCA data for non-cancerous renal tissue samples. The patients with RCCs were clustered into two subclasses, clusters A_N and B_N (Fig. 2a). The corresponding RCCs of patients in Cluster B_N showed more frequent macroscopically evident renal vein tumor thrombi, microscopically evident vascular involvement, and higher pathological TNM stages than those in Cluster A_N.[72] The overall survival rate of patients in Cluster B_N was significantly lower than that of patients in Cluster A_N (Fig. 2a).[72] Tumor aggressiveness and even patient outcome might thus be determined by DNA methylation profiles at the precancerous stage.

In RCCs themselves, more BAC clones showed DNA hypo- or hypermethylation, and its degree was increased in comparison with samples of non-cancerous renal tissue obtained from patients with RCCs. Two-dimensional unsupervised hierarchical clustering analysis based on BAMCA data for RCCs was able to group patients into two subclasses, Clusters A_T and B_T (Fig. 2a). RCCs in Cluster B_T more frequently showed renal vein tumor thrombi, vascular involvement, and higher pathological TNM stages than those in Cluster A_T.[72] The overall survival rate of patients in Cluster B_T was significantly lower than that of patients in Cluster A_T (Fig. 2a).[72]

Patients who were grouped in Cluster B_N on the basis of BAMCA data for non-cancerous renal tissue were also grouped in Cluster B_T on the basis of BAMCA data for RCC themselves. That is, Cluster B_N was completely included in Cluster B_T (Fig. 2b).[72] The majority of the BAC clones significantly discriminating Cluster B_N from Cluster A_N also discriminated Cluster B_T from Cluster A_T.[72] Among BAC clones characterizing both clusters B_N and B_T, where the average signal ratio of Cluster B_N was higher than that of Cluster A_N, the average signal ratio of Cluster B_T was also higher than that of Cluster A_T without exception (Fig. 2b). Among BAC clones characterizing both clusters B_N and B_T, where the average signal ratio of Cluster B_N was lower than that of Cluster A_N, the average signal ratio of Cluster B_T was also lower than that of Cluster A_T without exception (Fig. 2b). Comparison between the signal ratios of each BAC clone characterizing both clusters B_N and B_T in non-cancerous renal tissue and those in the corresponding RCCs for all patients revealed that the DNA methylation status of the non-cancerous renal tissue was basically inherited by the corresponding RCC in each individual patient (Fig. 2b).[72]

In non-cancerous renal tissue showing no remarkable histological changes and consisting mainly of renal tubules with specialized functions, no progenitor cell is able to gain a growth advantage, and clonal expansion is unable to occur. Therefore, the distinct DNA methylation profile of Cluster B_N, which is clinicopathologically valid, cannot be established through the selection of one of a number of random DNA methylation profiles in non-cancerous renal tissue in patients with clear cell RCCs, and instead may be established through distinct target mechanisms. As the DNA methylation profiles in Cluster B_T are shared by phenotypically similar patients, who all suffer from clinicopathologically aggressive tumors and show a poor outcome, DNA methylation alterations in at least a proportion of the BAC regions characterizing Cluster B_T cannot be passenger changes. It is clear that cancer itself can induce alterations in DNA methylation. However, DNA methylation alterations of BAC regions characterizing Cluster B_T may significantly participate in carcinogenesis, as the DNA methylation profile in Cluster B_N was established at a very early and precancerous stage of carcinogenesis and inherited during progression of the cancers themselves as Cluster B_T. At least a proportion of DNA methylation alterations at the precancerous stage may be "epigenetic gatekeepers"[21] and which allow time for further epigenetic and genetic alterations including genetic gatekeeper mutations (Fig. 3).

In fact, when the DNA methylation status of C-type CpG islands was examined,[73] the average number of methylated

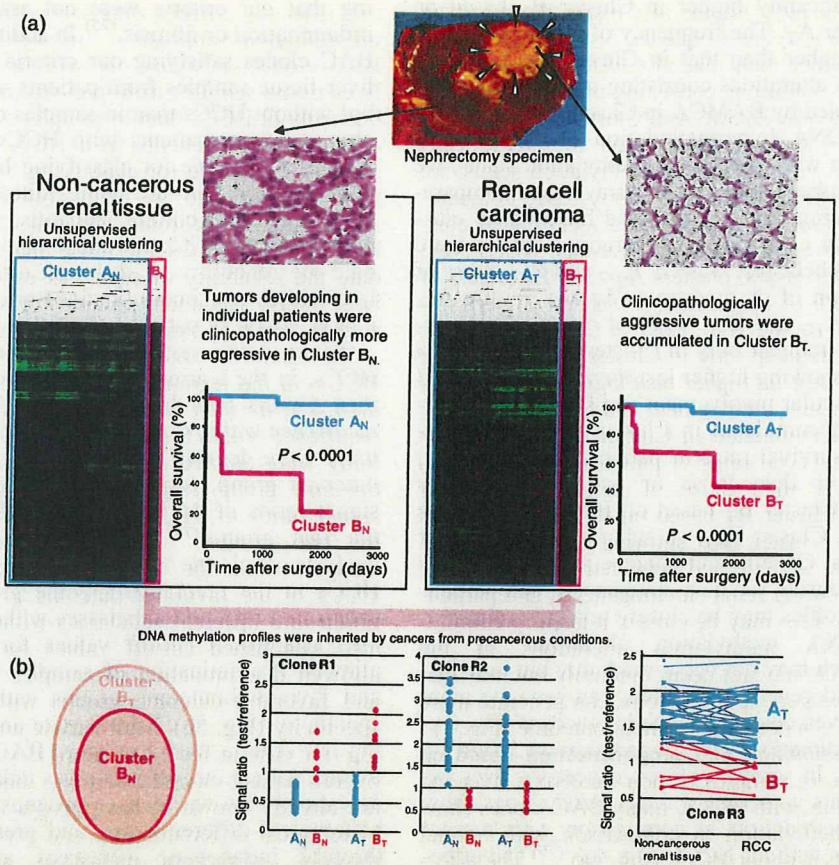

Fig. 2. DNA methylation profiles in precancerous conditions and renal cell carcinomas (RCCs). (a) Bacterial artificial chromosome array-based methylated CpG island amplification (BAMCA) data for tissue samples obtained from patients with RCCs (arrowheads). Using unsupervised hierarchical clustering analysis based on BAMCA data for samples of their non-cancerous renal tissue, patients with RCCs were clustered into two subclasses, Clusters A_N and B_N.[72] Clinicopathologically aggressive RCCs were accumulated in Cluster B_N, and the overall survival rate of patients in Cluster B_N was significantly lower than that of patients in Cluster A_N.[72] Using unsupervised hierarchical clustering analysis based on BAMCA data for their RCCs, patients were clustered into two subclasses, Clusters A_T and B_T.[72] Clinicopathologically aggressive clear cell RCCs were accumulated in Cluster B_T, and the overall survival rate of patients in Cluster B_T was significantly lower than that of patients in Cluster A_T.[72] (b) Correlation between DNA methylation profiles of precancerous conditions and those of RCCs. Cluster B_N was completely included in Cluster B_T (left panel). The majority of the bacterial artificial chromosome (BAC) clones, 724 in all, significantly discriminating Cluster B_N from Cluster A_N, also discriminated Cluster B_T from Cluster A_T.[72] In 311 of the 724 BAC clones, where the average signal ratio of Cluster B_N was higher than that of Cluster A_N, such as Clone R1 in the middle panel, the average signal ratio of Cluster B_T was also higher than that of Cluster A_T without exception.[72] In 413 of the 724 BAC clones, where the average signal ratio of Cluster B_N was lower than that of Cluster A_N, such as Clone R2 in the middle panel, the average signal ratio of Cluster B_T was also lower than that of Cluster A_T without exception.[72] As shown in the scattergram of the signal ratios in non-cancerous renal tissue samples and RCCs for all examined patients for a representative BAC clone, Clone R3, the DNA methylation status of the non-cancerous renal tissue was basically inherited by the corresponding RCC in individual patients (right panel).[72]

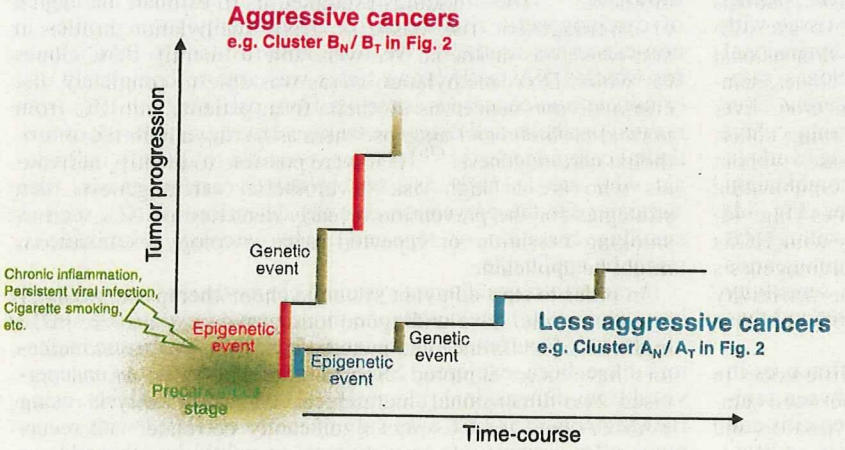

Fig. 3. Significance of DNA methylation alterations at the precancerous stage. Chronic inflammation, persistent infection with viruses or other pathogenic microorganisms, cigarette smoking, exposure to chemical carcinogens, and other unknown factors may participate in the establishment of particular DNA methylation profiles, such as Cluster B_N in Fig. 2. Such DNA methylation alterations in precancerous conditions may not occur randomly, but may be prone to further accumulation of epigenetic and genetic alterations (regional DNA hypermethylation of C-type CpG islands and copy number alterations were accumulated in Cluster B_T in Fig. 2),[72] thus generating more malignant cancers, such as the renal cell carcinomas in patients belonging to Cluster B_T.

doi: 10.1111/j.1349-7006.2009.01383.x